Short title

AI and HTP for GWAS and TWAS of WUE in sorghum

Corresponding author

Andrew D.B. Leakey, leakey@illinois.edu

Article title

Machine learning enabled phenotyping for GWAS and TWAS of WUE traits in 869 field-grown sorghum accessions

All author names and affiliations

John N. Ferguson[1,8]*, Samuel B. Fernandes[1]*, Brandon Monier[4], Nathan D. Miller[7], Dylan Allan[1], Anna Dmitrieva[1], Peter Schmuker[1], Roberto Lozano[5], Ravi Valluru[4,9], Edward S. Buckler[4,5,6], Michael A. Gore[5], Patrick J. Brown[1,10], Edgar P. Spalding[7], & Andrew D.B. Leakey[1,2,3]

[1]Institute for Genomic Biology, [2]Department of Crop Sciences, and [3]Department of Plant Biology University of Illinois at Urbana-Champaign, Urbana, Illinois 61901

[4] Institute for Genomic Diversity, [5]Plant Breeding and Genetics Section, and [6]School of Integrative Plant Science, Cornell University, Ithaca, New York 14853

[7]Department of Botany, University of Wisconsin, Madison, Wisconsin 53706

[8]Current address: School of Biosciences, University of Nottingham, Sutton Bonington Campus, Sutton Bonington, Leicestershire LE12 5RD, UK

[9]Current address: Lincoln Institute for Agri-Food Technology, University of Lincoln, Lincoln, LN2 2LG, UK

[10]Current address: Section of Agricultural Plant Biology, Department of Plant Sciences, University of California Davis, California 95616

*Equal contribution

ORCIDs: 0000-0003-3603-9997 (J.N.F), 0000-0003-1332-711X (P.J.B.), 0000-0001-6251-024X (A.D.B.L)

One sentence summary: Rapid phenotyping and machine learning enabled GWAS and TWAS of stomatal density, specific leaf area and photosynthetic gas exchange in 869 field-grown accessions of biomass sorghum in wet and dry years.

ABSTRACT

Sorghum is a model C4 crop made experimentally tractable by extensive genomic and genetic resources. Biomass sorghum is also studied as a feedstock for biofuel and forage. Mechanistic modelling suggests that reducing stomatal conductance (g_s) could improve sorghum intrinsic water use efficiency (*iWUE*) and biomass production. Phenotyping for discovery of genotype to phenotype associations remain bottlenecks in efforts to understand the mechanistic basis for natural variation in g_s and *iWUE*. This study addressed multiple methodological limitations. Optical tomography and a novel machine learning tool were combined to measure stomatal density (SD). This was combined with rapid measurements of leaf photosynthetic gas exchange and specific leaf area (SLA). These traits were then the subject of genome-wide association study (GWAS) and transcriptome-wide association study (TWAS) across 869 field-grown biomass sorghum accessions. SD was correlated with plant height and biomass production. Plasticity in SD and SLA were interrelated with each other, and productivity, across wet versus dry growing seasons. Moderate-to-high heritability of traits studied across the large mapping population supported identification of associations between DNA sequence variation, or RNA transcript abundance, and trait variation. 394 unique genes underpinning variation in WUE-related traits are described with higher confidence because they were identified in multiple independent tests. This list was enriched in genes whose orthologs in Arabidopsis have functions related to stomatal or leaf development and leaf gas exchange. These advances in methodology and knowledge will aid efforts to improve the WUE of C4 crops.

INTRODUCTION

Global climatic change is subjecting agricultural regions to elevated atmospheric vapor pressure deficits (VPD; Yuan et al., 2019) and reduced precipitation events (Sheffield and Wood, 2008), thereby giving rise to situations where more water is needed, but less is available. Water use efficiency (WUE; the ratio of carbon gain to water loss) is a key target trait for crop improvement to improve production and sustainable water use (Bailey-Serres et al., 2019; Leakey et al., 2019). C_4 crops including maize, sorghum, sugarcane, millet and Miscanthus are heavily studied as sources of food, feed, fuel and fiber. However, less research has been directed towards understanding and improving WUE and its component traits in C_4 crops, possibly because they already achieve high WUE as a result of the CO_2 concentrating mechanism they possess (DeLucia et al., 2019). Nevertheless, mechanistic modeling suggests that enhancing intrinsic WUE (*iWUE*) by reducing stomatal conductance (g_s) while maintaining rates of net CO_2 assimilation (A_N) can increase biomass production in C_4 as well as C_3 species across a broad range of environmental conditions (Truong et al., 2017; Leakey et al., 2019). These benefits will become greater as atmospheric [CO_2] continues to rise. Compiling surveys of natural variation in C_4 species, including grain sorghum (Kapanigowda et al., 2013), demonstrated that g_s could explain substantially more variation in *iWUE* than A_N (Leakey et al., 2019).

Sorghum is a model C_4 crop made experimentally tractable by extensive genomic and genetic resources (Paterson et al., 2009; Morris et al., 2013). And, biomass sorghum has considerable potential as a biofuel feedstock in addition to being grown for forage (Castro et al., 2015). This study aimed to address key knowledge gaps regarding natural variation in *iWUE* and related traits across diverse biomass sorghum accessions, including evaluation of heritability, environmental effects, trait correlations, and associations between DNA sequence variation or RNA transcript abundance and trait values. *iWUE* was studied alongside its component traits (A_N and g_s) plus stomatal density (SD) and specific leaf area (SLA), because these anatomical and allometric traits are known to influence leaf physiology.

Stomata open and close to regulate the rate of CO_2 and water vapor exchange between leaves and the atmosphere (Cowan and Farquhar, 1977). These fluxes are also influenced by the size and density of stomata (Franks and Beerling, 2009; Dow et al., 2014). Empirical data shows that SD is positively correlated with g_s in a number of species (Anderson and Briske, 1990; Pearce et al., 2006). Molecular mechanisms controlling stomatal morphology and patterning have been elucidated in *Arabidopsis thaliana* (Chater et al., 2017). This has been combined with understanding of how g_s and WUE are linked to stomatal physiology to develop C_3 plants with improved WUE. For example, the expression of species-specific orthologs of the *A. thaliana EPIDERMAL PATTERNING FACTOR 1* (*EPF1*) gene has been targeted to reduce g_s through reduced SD, thereby improving WUE in barley (Hughes et al., 2017), rice (Caine et al., 2019; Mohammed et al., 2019), wheat (Dunn et al., 2019) and poplar (Wang et al., 2016). The majority of cultivated crops are grasses (Leff et al., 2004). Stomatal morphology and development in grasses is markedly different from that of dicotyledonous species, e.g. *A. thaliana*, and reflects specific selective pressures (Hetherington and Ian Woodward, 2003). Consequently, whilst in some instances the molecular underpinnings of these traits are conserved between *A. thaliana* and grasses (Hughes et al., 2017; Caine et al., 2019; Dunn et al., 2019; Mohammed et al., 2019), emerging evidence suggests the biological functioning of key stomatal genes can be divergent between the lineages (Raissig et al., 2017; Abrash et al., 2018). As such, improving our understanding of grass-specific genes that regulate stomatal development and patterning will expedite efforts to improve WUE in crops. The need to address this knowledge gap is greatest in C_4 species.

SLA is the ratio of leaf area to leaf mass, which combines information on leaf thickness and leaf density (John et al., 2017). It is a key trait in the leaf economic spectrum than influences many traits including photosynthesis, respiration, leaf construction costs, leaf life span, canopy light interception and growth rates (Wright et al., 2004). Despite its importance, and that it can be measured easily, efforts to understand the genetic architecture of the trait through quantitative trait loci mapping or GWAS have been limited (Yin et al., 1999; El-Lithy et al., 2004; Trachsel et al., 2010). But, correlations between SLA and SD have been observed in response to varying

116 water supply (Xu and Zhou 2004) and across intraspecific variation associated with adaptation
117 to aridity (Carlson et al., 2016). The genetic and environmental control of SLA and its
118 relationship to SD in C_4 species is especially poorly understood.
119
120 Efforts to discover the genetic basis of traits that influence the sustainability and resilience of
121 crop productivity, including *iWUE*, are constrained by bottlenecks in both phenotyping as well
122 as discovery of associations between trait variation and DNA sequence variation or gene
123 expression (Yang et al., 2020). Automation, remote sensing and machine learning are
124 increasingly being used to accelerate the measurement and/or quantification of key
125 ecophysiological traits (e.g. Atkinson *et al.* 2017; Banan *et al.* 2018; Feldman *et al.* 2018; Qiao *et*
126 *al.* 2019). Optical tomography has been proposed as a method for imaging cell patterning on
127 leaf surfaces that is much more rapid than traditional methods of epidermal peels or imprinting
128 (Haus et al., 2015). Identifying and counting stomatal complexes on the epidermis is the most
129 time-consuming aspect of screening SD. A number of machine learning tools have been
130 proposed for counting stomata (e.g. Fetter et al., 2019; Li et al., 2019; Sakoda et al., 2019).
131 However, proof of concept is still required for the use of optical tomography and an automatic
132 stomatal counting tool suitable for use across the phenotypic variation associated with diverse
133 genotypes of a grass species.
134
135 Genome-wide or transcriptome-wide association studies (GWAS and TWAS) are popular
136 methods that can identify genomic regions or genes for which variation in DNA sequence or
137 gene expression is associated with quantitative variation in a trait of interest (Tian et al., 2011;
138 Hirsch et al., 2014; Xu et al., 2017). The challenges associated with phenotyping traits
139 associated with *iWUE* in C_4 crops mean that these methods have only been applied in a limited
140 number of cases (Ortiz et al., 2017; Feldman et al., 2018, Ellsworth et al., 2020). But, even when
141 phenotypic data is readily available, association studies are often challenging because many
142 traits are highly polygenic, where a large number of genes each exert a weak effect on the trait
143 (Zhu et al., 2008). Larger mapping population sizes can improve statistical power to counteract
144 this problem. But, multiple testing at many single nucleotide polymorphisms across the genome

145 also creates a significant risk of false positive results. Validating the function of candidate genes
146 via reverse genetics remains the gold standard, but is extremely slow. Approaches that can
147 increase confidence and efficiency of identification of candidate genes from association studies
148 are therefore important. One simple approach is to prioritize genes identified in multiple
149 independent tests. Alternatively, GWAS can be supplemented by TWAS. Most recently, proof-
150 of-concept for applying Fisher's combined test to integrate GWAS and TWAS was provided by
151 demonstrating how it increased the efficiency with which known causal genes could be "re-
152 discovered" for well-studied maize kernel traits (Kremling et al 2019). However, the application
153 of the method to address knowledge gaps for traits such as *iWUE* is untested.
154
155 In summary, to address knowledge gaps about the physiology and genetics of natural variation
156 in *iWUE* in C_4 grasses, this study evaluated a diverse population of 869 biomass sorghum
157 accessions grown in replicated trials over two growing seasons. To achieve this goal, a set of
158 novel tools were developed, tested and integrated. To break the phenotyping bottleneck for
159 SD, optical tomography was adapted and tested as an imaging technology and a custom
160 machine learning software platform was developed to automatically identify and count
161 stomatal complexes. This was combined with a rapid method to measure leaf-level gas
162 exchange and specific leaf area (SLA). Trait correlations were evaluated and genes putatively
163 underlying genetic variation in *iWUE* and related traits were identified through GWAS, TWAS
164 and an ensemble association mapping approach.
165
166
167

RESULTS

Growing season climate

A diversity panel of 869 photoperiod-sensitive sorghum accessions (Figure S1; Table S1) was grown at field locations within a five-km radius in 2016 (N=2; Fisher and Energy Farms) and 2017 (N=2; Maxwell and Energy Farms). Mean daytime maximum temperature was similar between 2016 (28.9 ˚C) and 2017 (28.8 ˚C). But, compared to the average growing season rainfall of 396 mm (Gelaro et al., 2017), 2017 was dry (174 mm) and 2016 was wet (529 mm; Figure S2).

High-throughput phenotyping metrics

A high-throughput approach for measurement of photosynthetic gas exchange (g_s, A_N, *iWUE*, and the ratio of intracellular to atmospheric CO_2 concentration (c_i/c_a)) along with tissue sampling for SLA and SD was performed on ~220 leaves per day, allowing two leaves per replicate plot of every genotype in the population to be sampled through 9-10 days of work for each replicate field in a given year.

Optical topometry (OT) was used to rapidly image 4-6 fields of view (FOV) from the abaxial surface of 4169 leaves in 2016 and 3211 leaves in 2017 without the need for sample preparation beyond adhesion to microscope slides with double-sided tape (~250 FOVs per day per OT microscope; Figure 1A). High-throughput computing resource allowed SD to be assessed for each of the 33,355 FOVs in <24 hours using a convolutional neural network that was trained to identify stomatal complexes in a rotationally invariant manner (Figure 1B; Figure S3). In contrast, based on recent experience, manual counting of this image set would take an estimated 80 person-days. The median SD per leaf generated by this machine-vision platform was significantly positively correlated (R^2 = 0.72, p<0.001) with the median SD per leaf from human counting of 228 randomly selected ground truth samples (Figure 1C). Although, there was a bias towards overestimation of SD by the computer as a result of a low rate of false positive identification of cells as stomatal complexes, especially on leaves with lower stomatal density.

Natural variation of WUE associated traits

Under the drought conditions of 2017, SD was 40% lower on average than in wetter conditions of 2016 (Figure 2A). The range of trait variation was also 26% less in 2017 than 2016. In contrast, SLA was 24% greater, on average, in 2017 than 2016. Again, this was associated with less variation within the population in the drought year (Figure 2B). Leaf photosynthetic gas exchange was only measured in 2017. On a relative basis, the observed variation in trait values was greatest for g_s (0.17 to 0.41 mol m^{-2} s^{-1}) and A_N (19.8 to 35.0 µmol m^{-2} s^{-1}), moderate for SD and SLA in the same year, and least for *iWUE* (108 - 151 µmol mol^{-1}) and c_i/c_a (0.40 – 0.52; Figure 2C-F). Plant height was strongly correlated between 2016 and 2017 (r = 0.94; Figure S15). Therefore, adjusted genotypic means were calculated for plant height from a mixed model incorporating data from both 2016 and 2017 at the growth stage where heritability was highest (height-joint; Figure 2G). The mean height-joint was 302 cm and varied within the population from 143 to 381 cm. Plant biomass was only measured in 2017. Mean biomass production was 28.7 t ha^{-1} (Figure 2H).

SD in 2016 was significantly correlated with SD in 2017 to a moderate degree (r = 0.36; Figure 3, see Table S2 for details). Variation among the population in SLA was slightly more consistent across wet and dry growing conditions, resulting in a stronger correlation in SLA between 2016 and 2017 (r = 0.46; Figure 3). Plant height was also positively correlated with above-ground biomass production in 2017 (Figure 3).

SD in 2016, 2017, and when genotypic means for SD were calculated in a joint model incorporating data from both years (SD-joint), were not significantly correlated with g_s, *iWUE* or c_i/c_a (Figure 3). However, SD in 2016 and SD-joint were weakly negatively correlated with A_N in 2017. And, SD was weakly negatively correlated with SLA within each of the two growing seasons. All three SD traits were positively correlated with height. Similarly, SD in 2016 and the SD-joint were positively correlated with biomass production in 2017. The relative change in SD

between growing seasons varied from -9 to -47 %, and was weakly, positively correlated with biomass production and height (Figure 3).

A_N and g_s were positively correlated with each other (Figure 4A). A_N and g_s were both negatively correlated with *iWUE*, but g_s explained more than twice as variation in iWUE (R^2 = 0.69) than A_N (R^2 = 0.32; Figure 4B, C). *iWUE* was weakly positively correlated with biomass production in 2017, but was not correlated with height. *iWUE* was also positively correlated with all SLA traits, with the relationship being strongest for SLA measured in the same growing season as the photosynthetic gas exchange i.e. 2017.

To varying degrees in each year, SLA in 2016, 2017 and SLA-joint were all negatively correlated with A_N, g_s, c_i/c_a, SD, and height. The relative change in SLA between growing seasons varied from -2 to +34 %, and was positively correlated with the relative change in SD between growing seasons as well as height, SD in 2016 and iWUE.

Genetic basis of WUE associated traits

Generalized heritability, was relatively high for SD and SLA (Figure 5). However, the heritability for SD in 2017 (0.50) was lower than in 2016 (0.68) and for SD-joint (0.69). In contrast, heritability for SLA-joint (0.80) was greater than for the individual years of 2016 (0.68) and 2017 (0.71). Leaf-level gas exchange traits demonstrated low to moderate heritability (g_s = 0.44, A_N = 0.42, *iWUE* = 0.31, c_i/c_a = 0.26).

A three-tiered approach for genetic mapping was used to identify candidate genes underlying the variation observed for the WUE-associated traits under study. Adjusted genotypic means from each linear mixed model for each trait were used for a genome-wide association study (GWAS; e.g. Figure 6A). The genes within linkage disequilibrium (LD) of the most statistically significant 0.1% of GWAS SNPs (Table S3) were then identified (Table S4). The number of independent genes identified per trait varied from 475 for SLA in 2016 to 656 for A_N in 2017 (Figure 6F; Figures S4 – S13). The 1% of gene transcripts that had the most statistically

significant associations with a given trait (Table S5; Figure 6B and C; Figures S4 – S13) were identified in transcriptome-wide association studies (TWAS) performed independently for the shoot growing point (GP; 195 genes per trait) as well as the developing third leaf (3L; 167 genes per trait). The p-values for these lists of "top hit" genes identified by GWAS and TWAS were integrated via the Fisher's combined probability test to identify candidate genes that the two orthogonal tests suggest underlie the observed phenotypic variation across the population (Table S6; Figure 6D and E; Figures S4 – S13).

Candidate genes identified in two or more independent tests are less likely to be false positives i.e. more likely to be associated with genetic variation in the traits of interest. Therefore, the consistency in results was tested: (a) across test types for a single trait (Figure 7A); and (b) across key trait groups, years or test-types (Figure 7A). Between 37 and 59 candidate genes were identified with high confidence for a given trait, based on being identified in at least two independent tests (Figure 7A, Figure 6, Figures S4-S12, Tables S7 and S8). This criterion was most consistently met when the tests integrated data about trait associations with both DNA sequence and RNA transcript abundance, and did so for transcript abundance in both the developing leaf (3L) and growing point (GP) (Figure 7A). For example, 48 genes in total met this criteria for SD in 2016 (Figure 6F) by being consistently identified by: both Fisher's tests (12 genes), both Fisher's tests plus both TWAS tests (2 genes), both Fisher's tests plus one TWAS test (3 + 1 genes), both Fisher's test plus the GWAS (29 genes), or a Fisher's test and both TWAS tests (1 gene). In addition, a moderate number of high confidence genes were identified when the tests integrated data about trait associations with DNA sequence and RNA transcript abundance in a single tissue (Figure 7A). For example, 7 genes met this criteria for SD in 2016 by being consistently identified by the GWAS and TWAS (1 gene) or GWAS, TWAS and Fisher's test (4 + 2 genes) for a given tissue (Figure 6F). The smallest number of "high confidence" genes were found by being identified in TWAS tests for both tissues, without evidence for genotype to phenotype associations from GWAS (Figure 7A). For example, 2 genes met this criteria for SD in 2016 (Figure 6F). These patterns were consistent for all the traits tested. When compiled across all the leaf traits, these multiple independent tests identified 394 unique candidate genes for

associations with trait variation for RNA plus DNA, or from both tissues where the transcriptome was tested (Figure 7B, Table S7 and S8).

Candidate genes were also consistently identified by two or more tests that spanned key trait groups (Figure 7B). For example, 213 genes were independently identified by tests for both SD and SLA. 280 genes were independently identified by tests for both SD and photosynthetic gas exchange traits. 288 genes were independently identified by tests for both photosynthetic gas exchange traits and SLA. Comparing across independent tests in separate growing seasons, 72 genes associated with variation in SD were consistently identified in 2016 and 2017. While 69 genes associated with variation in SLA were identified in both years.

In at least 75 cases, the orthologs in Arabidopsis of candidate genes identified here are annotated by TAIR (www.arabidopsis.org) as having some function related to leaf development or WUE (Table S9 and references therein). For example, AT3G06129 (MUTE) shares the greatest sequence similarity with Sobic.009G260200 identified for SD, and enocdes a bHLH protein that controls meristemoid differentiation during stomatal development (Kim et al 2012). AT1G51660 (MAPK4) is most similar to Sobic.004G323600 identified for g_s and is disease resistance protein involved in ABA-regulated stomatal movements (Hettenhausen, Baldwin & Wu 2012; Witoń *et al.* 2016). AT4G00430 (PIP1;4) is most similar to Sobic.006G176700 identified for A_N and is CO2 transporter involved in photosynthetic metabolism (Li et al., 2015).

DISCUSSION

The trade-off between carbon gain and water use is a fundamental constraint for crop productivity and environmental resilience (Bailey-Serres et al., 2019; DeLucia et al., 2019; Leakey et al., 2019). More specifically, improving WUE is recognized as a means to enhance the utility of sorghum as a biofuel feedstock (Mathur et al., 2017; Meki et al., 2017). Nevertheless, understanding of genetic variation in traits that underlie iWUE in C_4 grasses is poor even after more than a century of WUE research (Briggs and Shantz 1917; Leakey et al., 2019). This study successfully met the goal of developing an integrated approach for rapid *iWUE* phenotyping. And, it used these technical advances to provide one of the largest and most comprehensive investigations of genetic and environmental variation in leaf traits that influence WUE, i.e. g_s (Hatfield and Dold, 2019; Leakey et al., 2019), A_N (Hatfield and Dold, 2019; Leakey et al., 2019), SD (Bertolino et al., 2019), and SLA (Zhang et al., 2009; Zhang et al., 2015). A novel element of that investigation was integration of GWAS and TWAS to identify candidate genes that can be further studied to understand and improve *iWUE* in sorghum and other C_4 crops.

Rapid Phenotyping

Traditional assessments of traits relating to leaf gas exchange and stomatal patterning are time and labor intensive. For example, measuring light saturated gas exchange of individual leaves can take >30 minutes (Ortiz et al., 2017; Qu et al., 2017) and manually peeling leaf epidermal samples and counting stomata via light microscopy is slow (Yates et al., 2018). Consequently, these traditional approaches are not readily amenable to large-scale assessments of genetic variation. A high-throughput phenotyping pipeline (Figure S13) was developed by integrating: (a) a rapid method of measuring leaf-level gas exchange (Figure S14; Choquette et al., 2019); b) rapid scanning of abaxial leaf surfaces and automated stomatal counting (Figures 1, S3); and c) sampling for SLA. Over 200 leaves were processed per day, facilitating phenotyping of 869 accessions replicated across two field trials in each year. This was a substantial gain in scale over previous experiments looking at similar traits in isolation (Taylor et al., 2016; Ortiz et al., 2017; Herritt et al., 2018; Lü et al., 2018; Yates et al., 2018). Our automated approach for determining SD was validated by comparisons to ground truth data (Figure 1C). And, computer-

based measurement of SD in 33,355 FOV was approximately 80 times faster than counting of stomatal complexes by humans. Importantly, the efficacy of the method across a wide range of genetic and environmental variation in epidermal leaf anatomy was highlighted by the moderate-to-high heritability of SD (Figure 5). These heritability estimates were similar or higher than those previously reported (e.g. Delgado et al., 2011; Dittberner et al., 2018). A variety of machine learning methods have been developed that can identify stomata in images (e.g. Aono et al., 2019; Fetter et al., 2019; Li et al., 2019), but demonstrations of their applicability to large-scale genetic studies of the measured trait are rare (Dittberner et al., 2018) to non-existent depending on the species. Overall, this work along with Xie et al., (in review) and Bheemanahalli et al., (in review) demonstrates the utility of optical tomography and computer-vision as tools that can meet the potential for accelerating biological discovery in cereal crops.

Genetic variation in *iWUE*, A_N and g_s

We detected a positive association between A_N and g_s (Figure 4). This is consistent with previous studies of diverse germplasm in C_4 crops, such as maize (Choquette et al., 2019), sugarcane (Inman-Bamber et al., 2016), and switchgrass (Taylor et al., 2016). And, it affirms that accessions with greater g_s achieve greater rates of A_N, despite sorghum having a biochemical pump concentrating CO_2 around Rubisco in the bundle sheath cells. However, the non-linear nature of the relationship also indicates diminishing returns from greater g_s in terms of A_N, leading to lower *iWUE* among accessions with the greatest g_s. Selection for greater productivity in other crops has been associated with greater g_s and water use (Roche 2015, Koester et al., 2016). Repeating the same strategy would not be desirable in sorghum, assuming that high productivity under water-limited conditions is a priority. Notably, the genetic variation observed in *iWUE* was more a factor of variation in g_s (Figure 4C) than variation in A_N (Figure 4B). Taken together these results demonstrate that enhanced *iWUE* is achieved either through low g_s or through coupling high A_N with moderate g_s. While in the past it was suggested that WUE across C_4 species was almost invariant (DeLucia et al., 2019), this study builds on work in sugarcane (Inman-Bamber et al., 2016) to suggest that meaningful variation does exist. Our

generalized estimates of heritability for A_N and g_s (Figure 5) were similar to those estimated in a recent survey of the same traits in a smaller panel of grain sorghum accessions (Ortiz et al., 2017) and sufficiently high to justify targeting them as traits for selection. But, efforts to improve WUE in sorghum via direct selection on *iWUE* may inadvertently limit A_N in the same way as previously observed in C3 crops (Condon et al., 2004; Leakey et al., 2019). So, understanding a broader set of component traits that influence *iWUE* will be valuable.

Contrary to theoretical expectations, and prior observations in grass crops (Miskin et al., 1972; Muchow and Sinclair, 1989; Panda et al., 2018), there was no significant correlation between SD and leaf gas exchange traits across the diverse panel of sorghum accessions (Figure 3). This was also the case in maize RILs (Xie et al., in review). But, detecting an association between SD and g_s may be complicated by a strong trade-off between SD and stomatal size (Xie et al., in review). The width and length of stomatal complexes were significantly correlated with leaf gas exchange traits in maize (Xie et al., in review). Stomatal length has been observed to positively correlate with g_s across rice accessions, where SD did not (Ohsumi et al., 2007). And, grain sorghum accessions selected for high or low SD alleles at a single locus display corresponding variations in g_s (Bheemanahalli et al., in review). Transgenic approaches to reducing SD have reduced g_s and increased *iWUE* in a number of crops (Wang et al., 2016; Hughes et al., 2017; Dunn et al., 2019; Mohammed et al., 2019). Therefore, advancing understanding of genes and traits associations underpinning SD and iWUE does have the potential to aid crop improvement efforts.

Genetic and environmental variation in SD and SLA

SD was significantly lower in the dry growing season of 2017 than the wet growing season of 2016 (Figure 2A). The morphology and patterning of stomata can be modified in developing leaves in response to environmental cues (Lake et al., 2001; Casson and Hetherington, 2010). Lower SD would tend to limit water loss via transpiration under dry conditions, consistent with many other mechanisms that operate to sense soil water content and conserve water (Franks and Farquhar, 2001; Chaves et al., 2009). However, the response of SD to limiting water supply

varies significantly among studies, species and with the intensity of drought stress (Quarrie and Jones, 1977; Hamanishi et al., 2012; Sakurai et al., 1986; Chaves et al., 2009). So, the consistent direction of response towards lower SD under drought conditions experienced in the field by this diverse sorghum population is noteworthy.

SLA was significantly greater, on average, in the drier growing season (Figure 2B), indicating an overall reduction in leaf thickness or density. SLA is well documented to demonstrate remarkable phenotypic plasticity in response to environmental stimuli (Hulshof et al., 2013; Wellstein et al., 2017). Depending on the prevailing conditions, SLA can be coupled to important functional traits, such as photosynthesis and growth rate (Pengelly et al., 2010; Liu et al., 2016; Wellstein et al., 2017; Gonzalez-Paleo and Ravetta, 2018), as well as water-use strategies and WUE (Wang et al., 2013; Scartazza et al., 2016).

Total canopy leaf area is likely to be more than sufficient to maximize light interception over most of the growing season in biomass sorghum. But, greater SLA allows greater leaf area to develop for a given investment in carbon resources. Therefore, it is possible that the greater SLA under drought conditions facilitated greater investment in other carbon sinks, such as root growth (Wellstein et al., 2017), thereby improving water uptake (Tardieu et al., 2017). Concurrently, the increase in SLA will have likely limited leaf-level carbon fixation (Xu and Zhou, 2008; Gonzalez-Paleo and Ravetta, 2018), due to a reduction in the thickness of the chloroplast-rich palisade mesophyll (Gonzalez-Paleo and Ravetta, 2018; Gotoh et al., 2018). This is reflected in the significant negative association observed between A_N and SLA in 2017 (Figure 3). Despite this reduction in leaf-level A_N, the side-effect of increased light penetration into the canopy may ameliorate losses in carbon gain at the canopy level (Evans and Poorter, 2001; Liu et al., 2016).

Plant height and biomass were positively correlated with the percentage change in trait values between growing seasons for both SD and SLA (Figure 3; Table S2). While many factors could contribute to this relationship, the most parsimonious explanation would be that more productive accessions generally have the greatest demand for water, exhaust available

resources to the greatest extent, and then demonstrate the greatest plasticity in anatomy and physiology required to avoid further drought stress. Further work is needed to understand the adaptive value of the observed plasticity for maintenance of productivity when water is limiting. It will also be important to learn if transgenic approaches to increasing *iWUE* via lower SD constrain plasticity under drought stress.

At the genetic level, understanding of the mechanisms determining SD and SLA have not been integrated. But, accessions displaying the greatest plasticity in SD tended to be more plastic in terms of SLA as well (Figure 3). A causal link between the two traits was not explicitly tested in the current study. But, the observed correlations are consistent with previous reports of greater leaf thickness enhancing the capacity for reductions in SD under drought (Galmés et al., 2007; Xu and Zhou, 2008). Lower SLA is widely associated with greater photosynthetic capacity (Wright et al 2004). And, theory dictates that greater maximum g_s, via greater SD or stomatal size, along with other aspects of hydraulic capacity in leaves should support greater exchange of water vapor for CO_2 to be assimilated through photosynthesis (Dow et al., 2014; Henry et al., 2019). This emphasizes the need to better integrate understanding of relationships of epidermal patterning with the anatomy and function of the leaf as a whole. Consequently, candidate genes associated with variation in both SD and SLA may be of special interest (Table S7, S8).

Combining GWAS and TWAS to identify candidate genes

The results of both GWAS and TWAS reinforced the prevailing understanding that *iWUE*, and associated leaf traits, are complex and polygenic (e.g. Des Marais et al., 2014; Ortiz et al., 2017; Dittenberger et al., 2018). As a consequence, and in common with many GWAS studies on a diverse range of traits (Zhu et al., 2008; Ortiz et al., 2017; Dittenberger et al., 2018; Kremling et al., 2019), many moderately significant associations were detected. This is consistent with individual alleles of small or moderate effect sizes segregating at moderate or low frequencies, respectively. In such cases, extra information is needed to avoid reporting false positive associations and boost confidence in the identification of candidate genes. This study provides

a demonstration of the concept tested by Kremling et al., (2019) where GWAS and TWAS are combined to achieve this goal. A total of 394 unique candidate genes were identified for the set of 10 leaf traits studied. To be included in this list a gene had to be identified for a given trait in multiple independent tests for either: (1) associations of trait variation with both RNA and DNA, or (2) associations of trait variation with transcript abundance in both tissue sample types (Figure 6, Figures S4-S12, Tables S7 and S8). This was the case for 37 – 59 genes per trait, with 80 genes meeting these criteria simultaneously for 2 or 3 traits. Detailed examination of the results on a trait-by-trait basis revealed the greatest consistency in results coming from the use of Fisher's combined test to integrate information from the GWAS with TWAS. But, there were examples where the same gene was identified from TWAS performed separately on transcriptome data from both tissue sample types (growing tip versus developing third leaf). In addition, confidence in the identification of other genes was greater because they were independently identified in both growing seasons (72 genes for SD and 69 genes for SLA) or they were identified for multiple traits resulting from independent measurements. The consistency across results for different types of traits in 2017 (213 genes for SD plus SLA; 280 genes for SD plus gas exchange traits; 288 genes for SLA plus gas exchange traits; Figure 7B) was than higher than for across growing seasons. But, this does not seem surprising given the difference in water availability between the two years and the potential for genotype x environment interactions. Confirmation of a role for these genes in driving variation in *iWUE* and related traits will still require a reverse genetics approach performed on a gene-by-gene basis. But, a significant number of the candidate genes identified are orthologs of genes in *A. thaliana* that have functions linked in some way to iWUE, A_N, g_s or leaf development and anatomy (Table S9). And, the preponderance of genes with associations between trait variation and transcript abundance may indicate that regulatory variation is a more common driver of genetic variation than sequence variants. It is worth noting that TWAS was performed using transcriptome data generated from plants in controlled conditions, as opposed to the field where phenotyping for GWAS was performed. Despite this, the molecular control of the physiological processes of interest is well conserved, which is reflected in the overlap of genes identified by association to RNA and DNA.

Candidate genes underlying variation in gas exchange and SD

In terms of genes identified underlying variation in g_s, but not A_N, *MAPK4*, identified via GWAS for g_s, represents a particularly promising candidate (Table S9). *MAPK4* is a well characterized disease resistance protein (Berriri et al., 2012), but evidence from aspen (Witoń et al., 2016) and agave (Sara et al., 2020) demonstrate a role for *MAPK4* in the regulation of g_s and stomatal development, which is in line with the identification of *MAPK4* via TWAS for SD in GP tissue also.

We did not observe strong associations between SD and gas exchange traits. This is possibly due to the restricted variation in SD in 2017. However, it is also likely due to the importance of further uncharacterized stomatal and mesophyll components for regulating gas exchange (Bertolino et al., 2019; Lawson and Matthews, 2020). Despite this, it is well understood that significantly manipulating SD can improve WUE in many species (Bertolino et al., 2019). Consequently, the candidate genes underlying SD identified in this study represent a starting point for future crop improvement to this end. Moreover, elucidating these candidates for their role in regulating SD may form the foundations of understanding stomatal development pathways in C_4 grasses.

Candidate SD genes with known roles in stomatal development included *MUTE*, which was identified via the Fisher test employing GP transcriptome data (Figure 6, Table S9). *MUTE* is a bHLH transcription factor that acts as a stoma-fate master regulator in dicots and monocots (Pillitteri et al., 2008; Raissig et al., 2017).

Further genes with demonstrated roles in stomatal development identified within this set included *KCS1* which controls stomatal patterning relative to CO_2 concentration (Gray et al., 2000) and *HB-7* which regulates stomatal size relative to water availability (Ré et al., 2014) (Figure 6, Table S9). Putative SD candidates in this gene set included a cell wall expansion-type protein (*EXPB2* (Marowa et al., 2016), an ABA-sensitive MAP KINASE (*RAF10* (Lee et al., 2015)),

the *PAP10* purple acid phosphatase (Hepworth et al., 2016), and an asparagine-rich protein (*NRP*) that is documented to positively regulate the expression of *CRY2* (Zhou et al., 2017), a blue light receptor which in turn increases stomatal index (Kang et al., 2009) (Figure 6, Table S9). Further genes with known roles in stomatal development identified via alternative mapping approaches included *AMP1* (Shi et al., 2013; López-García et al., 2020), *ATE1* (Movahedi, 2013; Vicente et al., 2019), and *TED5* (Tossi et al., 2014; Zoulias et al., 2020). Additionally, through mapping for SD we identified multiple genes with putative and known roles in stomatal behavior, e.g. the *CLC-C* anion transporter (Jossier et al., 2010), and ABA responsiveness, e.g. *FRS5* (Ma and Li, 2018), that represent interesting targets for further study.

CRR23 was identified via all mapping approaches for A_N (Table S9) and is known to be critical for stabilizing the chloroplast NAD(P)H dehydrogenase complex, thereby facilitating photosynthetic electron transport (Shimizu et al., 2008). The importance of this complex in controlling the observed variation in A_N was further highlighted by the identification of the *AOX1a* gene via multiple A_N mapping approaches (Table S9). *AOX1a* is well demonstrated to play a key role in electron transport and balancing the redox state of cellular NAD(P)H pools, thereby facilitating efficient photosynthetic functioning (Vishwakarma et al., 2014; Podgórska et al., 2020). Combined GWAS and TWAS for A_N also identified genes with demonstrated roles in chloroplast biosynthesis. For example, *PDS3* (Table S9) is a key component of retrograde signaling during chloroplast development. Indeed, *pds3*-mutants display an albino phenotype (Foudree et al., 2010). *PDS3* was also identified via mapping for g_s and SD, which is interesting since *PDS* genes have been implicated in ABA biosynthesis and the control of stomatal opening (Chao et al., 2014). *PIF3* represents a further candidate in this vein. *PIF3 w*as identified via mapping for A_N and g_s (Table S9). *PIF3* is a light-dependent transcriptional repressor of genes involved in chlorophyll biosynthesis and further photosynthetic processes (Liu et al., 2013). Additionally, the closely related *PIF4* gene has been demonstrated to regulate the expression of *SPEECHLESS* (*SPCH*), a master regulator of stomatal development (Casson et al., 2009; Lau et al., 2018), thereby hinting at a possible role in regulating g_s. Additionally, mapping for A_N identified *PIP1;4*

(Table S9), which is an aquaporin that regulates the permeability of the plasma membrane to CO_2, thereby mediating CO_2 transport for photosynthesis (Li et al., 2015).

CONCLUSION

This study demonstrates the application of novel high-throughput phenotyping tools with combined GWAS/TWAS to study the genetic basis for a challenging set of complex traits related to *iWUE* in a model C_4 crop. In doing so, it revealed heritable variation in multiple traits that selection could act upon to improve performance under water limited conditions. In addition, it highlights the central role that SLA may play as an allometric trait that is associated with broad genetic and environmental variation in SD, leaf photosynthetic gas exchange and plant productivity. Lastly, genomic and transcriptomic variation across this diversity set were leveraged to identify multiple candidate genes with known and putative roles for key WUE traits.

MATERIALS AND METHODS

Germplasm and experimental design

869 previously described biomass sorghum accessions (Valluru et al., 2019; Dos Santos et al., 2020) were used in this study (Figure S1; Table S1). All lines were grown during 2016 and 2017 across two field sites in Central Illinois (Savoy, IL), where experiments were sown in late May and harvested in late October. Lines were grown according to an augmented block design as reported previously (Valluru et al., 2019; Dos Santos et al., 2020).

High throughput phenotyping pipeline for WUE-associated traits

The youngest fully expanded leaf of two plants randomly selected from the middle two rows of each plot were excised slightly above the ligule between September 5 and 14, 2016. Damaged leaves were avoided. Excised leaves were immediately placed in a bucket, with the cut surface submerged under water. In the laboratory, three 1.6cm leaf discs were collected from each leaf while avoiding the midrib. Leaf discs were immediately transferred to an oven set at 60°C for

two weeks. The dry mass of leaf discs was determined and specific leaf area (SLA) was calculated as the ratio of fresh leaf area to dry leaf mass (cm^2 g^{-1}). The SLA data collected in 2016 were previously reported (Valluru et al., 2019).

A leaf tissue strip approximately 1cm x 3cm in area was also cut from the adjacent portion of the leaf from where the leaf discs were collected. Leaf strips were marked to distinguish the abaxial side, inserted into 2 mL screw cap tubes and flash frozen in liquid nitrogen and stored at -80°C. ~150 leaf strip samples were moved to -20°C during active microscopy. Leaf samples were removed from the -20℃ freezer and affixed to a microscope slide using double-sided tape with the abaxial side facing up. The surface topography of leaf surfaces was measured using two Nanfocus µsurf explorer optical topometers (Nanofocus, Oberhausen, Germany) at 20x magnification with a standardized area of 800 x 800 µm. The upper and lower z-scale limits being set manually for each FOV to ensure all stomata were in focus. The abaxial surface topography was measured at 4-6 randomly selected points producing 4-6 fields of view (FOV). . Measurements were saved in the .nms file format and automatically transferred for automated stomatal counting via a CyVerse-enabled data pipeline (Goff *et al.* 2011).

In 2017, leaf-level gas exchange of all accessions was measured in addition to sampling for SLA and tissue for stomatal imaging. The field was divided into four quartiles based on height measured in previous growing seasons. Each quartile was sampled over a 4- or 5-day period. On each measurement day, 200-232 leaves (2 leaves from 100-116 plots) were harvested pre-dawn as described for the 2016 SLA and SD leaf sampling. Upon returning the leaves to the lab, stable rates of light-saturated gas exchange were measured by following the experimental protocol described previously for maize (Choquette *et al.* 2019). Stable rates of net photosynthetic assimilation of CO2 (A_N), stomatal conductance (g_s), intrinsic water use efficiency (iWUE), and the ratio of intracellular and atmospheric CO2 (c_i/c_a) were obtained by averaging data from the last two minutes of a four-minute autolog program (Figure S14). After the measurements of leaf-level gas exchange, the area of the leaf contained within the cuvette was marked and used for sampling for leaf discs and tissues strips for subsequent measurements of SLA and stomatal

imaging as described above for the 2016 sampling campaign. A flow chart describing this pipeline is provided in Figure S13.

Automated stomatal counts

Image processing and machine learning methods were combined to produce a software tool that automatically detected stomata in 33,355 grayscale images of sorghum leaf surfaces. Constructing the method required a set of training data based on circular image disks 80 pixels in diameter centered where human experts had registered the locations of stomata in many 512x512 raw images. Each 80-pixel disk was subjected to circular fast Fourier transformation (FFT) to produce a radial series of phase and amplitude values that proved to be predictive of stomata. The radial FFT results were recast by principal components analysis (PCA) into a lower dimensional form that served as the feature set used to train nine different machine learning methods. The nine methods were: an Artificial Neural Network, Linear Discriminant Analysis, a Convolution Neural Network, three Generalized Linear Model's two Regularization (Ridge and Lasso) and one without, Partial Least Squares Regression, Stepwise Linear Regression and a Decision Tree. Each method produced a version of the original image in which each pixel value was a probability of that location belonging to a stoma. Next, a fusion process filtered and combined the independent probability maps such that local probability peaks in excess of a height threshold optimally coincided with the locations of human-verified stomata. Specifically, a Nelder-Mead optimization process adjusted the filter and threshold parameters to maximize the agreement between the machine-labeled stomata and the human-identified stomata as quantified by the Matthews correlation coefficient. Figure S3 shows an overview of the method. The analyses were implemented in the Matlab programming environment and deployed on a high throughput computing resource with jobs scheduled by HTCondor (Thain, Tannenbaum & Livny 2005). The machine learning and optimization processes (i.e. layers) were subsequently trained and tuned accordingly.

Each FOV from a stomatal imaging sample produced a stomatal count value. The stomatal count values were divided by the area of the images ($0.64mm^2$) to give stomatal density (SD). The median of the 4-6 SD estimates were calculated for each sample and used for subsequent

analyses. To benchmark the efficiency of the automated stomatal counting, we manually counted and estimated stomatal density for 227 randomly selected samples, which represented 1056 individual FOV. A linear model predicting manually counted stomatal density from automatic stomatal density was subsequently fit.

Plant height and biomass measurements

In 2016 and 2017, a single representative plant in each plot was measured for plant height as described and reported previously (Valluru et al., 2019; Dos Santos et al., 2020). For this study, plant height on 105 days after planting (DAP) was used for comparative analyses since it showed the greatest heritability of all days measured. In 2017, plants were harvested, and above ground biomass was measured and calculated as dry t ha-1 as previously described and reported (Dos Santos *et al.* 2020)

Statistical models and heritability

For each trait, we fitted a linear mixed model using the ASReml-R v4.0 package (Butler *et al*., 2018). The appropriate model was chosen based on the Akaike information criterion (AIC) and the diagnostic plots. As different covariables were evaluated along with each phenotype, the final model varied in each case (Table S10). The general model used was as follows:

$$\mathbf{y} = \mathbf{1}\boldsymbol{\mu} + \mathbf{X}_1\mathbf{t} + \mathbf{X}_2\mathbf{q} + \mathbf{Z}_1\mathbf{s} + \mathbf{Z}_2\mathbf{b} + \mathbf{Z}_3\mathbf{g} + \mathbf{Z}_4\mathbf{ge} + \mathbf{e}, \quad (1)$$

where **y** (n x 1) is the vector of phenotypes for j environments (year x location combination) with $n = \sum_{i=i}^{j} n_i$; **1** (n x 1) is a vector of ones; **μ** is the overall mean; $\mathbf{X}_1$ (n x j) is the incidence matrix associated with the vector of fixed effect environments **t** (j × 1); $\mathbf{X}_2$ (n x v) is the incidence matrix associated with the vector of fixed effect covariates **q** (v x 1) (see supplementary material for details on the number of fixed effects covariates used in each model, if any); $\mathbf{Z}_1$ (n x f) is the incidence matrix associated with the vector of random effect set within environment **s** (f x 1) with $s \sim MVN(0,\ I_f \otimes \boldsymbol{S})$; $\mathbf{Z}_2$ (n x r) is the incidence matrix associated with the vector of random block within set within environment effects **b** (r x 1) with

$b \sim MVN(0,\ I_r \otimes B)$; $\mathbf{Z}_3$ (n x l) is the incidence matrix associated with the vector of random genotype effects **g** (l x 1) with $g \sim MVN(0,\ I_l \otimes G)$; $\mathbf{Z}_4$ (n x w) is the incidence matrix associated with the vector of random genotype-by-environment effects **ge** (w x 1) with $ge \sim MVN(0, I_w \otimes K)$; and **e** (n × 1) is the vector of residuals with $e \sim MVN(0, \oplus_{i=1}^{j} I_{n_i} \otimes R_i)$. The matrices **S**, **B**, **G**, **K**, and **R** are the variance–covariance matrices for set within environment, block within set within environment, genotype, genotype-by-environment, and residual effects, respectively. For each genotype, we obtained predictions from model 1 and these were used for downstream analysis. The generalized heritability was estimated as proposed by (Cullis et al., 2006).

RNA-seq analysis

A subset of the full diversity panel was grown under controlled experimental conditions for 3' RNAseq analysis of genes potentially involved regulating leaf development, including stomatal patterning. The abundances of transcripts for orthologs of known stomatal patterning genes were initially screened across 3-7 separate tissues at each of 4 developmental stages during the day and night in six accessions. On the basis of that screen, the base of leaf three and the shoot growing point at the 3-leaf stage were targeted for sample collection during the day from a subset of 229 accessions from the full population. Samples were processed and expression data was generated from libraries using a pipeline and parameters similar to Kremling et al. (2019). Briefly, reads were trimmed using Trimmomatic (version 0.32) to remove adapter sequences in relation to *Illumina chemistry* and sequencing errors. Next, trimmed reads were aligned to the sorghum reference genome (version 3.1.1) using the splice-aware aligner, STAR (Spliced Transcripts Alignment to a Reference) (version 2.4.2). Feature counts were then generated using HTSeq (version 0.6.1) from previously generated alignment files. Finally, count normalization was performed using the R package, DESeq2 via size factor estimation.

GWAS

For conducting GWAS, we imputed the 100,435 GBS SNPs from (Dos Santos et al., 2020) using

as reference panel the whole-genome re-sequencing dataset of 5,512,653 SNPs published by Valluru et al. (2019). The untyped genotypes were imputed and phased into haplotypes using Beagle 4.1 using a default window size of 50,000 SNPs and an Ne = 150,000. After the imputation, SNPs with allelic R squared < 0.5 and minor allele count below 20 where removed, resulting in a total of 2,327,896 SNPs. Additionally, we pruned SNPs in high linkage disequilibrium (r^2> 0.9) using Plink options "--indep-pairwise 50 10 0.9". The final data set consisted of 454,393 SNPs scored in 836 sorghum lines.

The association analysis was conducted using the unified MLM (Yu et al. 2006) implemented in the software GEMMA (Zhou and Stephens, 2012). For that, predicted values obtained from model 1 were normal quantile transformed as done in (Zhou and Stephens, 2014). We used the Bayesian information criteria (BIC; Schwarz, 1978) to select the appropriate number of principal components (PCs) to account for population structure. We tested models with 0-10 PCs estimated from TASSEL 5 (Bradbury et al., 2007). The best model did not include any PC. Relatedness was controlled for by a kinship matrix obtained from TASSEL 5 using the default method (Endelman and Jannink, 2012).

TWAS and combined GWAS-TWAS

A transcriptome-wide association study (TWAS) was performed on a subset (229) of the total accessions (Valluru et al. 2019) and conducted using TASSEL (version 5.2.5). Before mapping, covariates were generated from multiple sources. 10 hidden factors were calculated using probabilistic estimation of expression residual (PEER) factors for each individual tissue (Stegle et al. 2012). Additionally, 5 genetic principal coordinates (PC) were calculated from prior genotype data (Valluru et al. 2019). Genes that were expressed in at least half of the individual lines were used within each tissue set. A general linear model was fit individually for each phenotype and every combination of expressed gene value across individuals after adjusting for PC and PEER factor covariates.

TWAS-GWAS combined p-values were calculated in a similar fashion as described by Kremling

et al. (2019). Briefly, p-values of the top 10 percent significant GWAS SNPs were assigned to their nearest gene. Assigned GWAS p-values were then combined with their respective TWAS p-values via the Fisher's combined test as using the sumlog function within the R package, metap.

To further explore the results of all genetic mapping approaches, we queried commonality between specific gene sets, e.g. genes identified for SD and SLA, SD genes common to 2016 and 2017, Genes identified via GWAS and Fisher's combined test, etc. (Figure 7B). For these comparisons, the total number of possible shared genes between any two gene sets was determined.

Candidate gene identification

For each GWAS result, the top 0.1% of SNPs based on $-\log_{10}(p\text{-}value)$ were identified. The linkage disequilibrium (LD) blocks these SNPs associated with was determined and all genes within these LD blocks or spanning their borders were extracted. LD blocks were estimated based on the method proposed by (Gabriel, 2002) and implemented in PLINK (Chang et al., 2015). For this, we used the option --blocks, with a window of 200 kb and default values for D-prime's confidence interval (0.7;0.98).

For the TWAS and the combined GWAS-TWAS, the top 1% of genes based on $-\log_{10}(p\text{-}value)$ were identified for each result. A list of candidate genes with known or putative roles in associated traits was determined based on overlap between different mapping approaches and/or traits.

Additional statistical analysis and figure generation

All further statistical analysis and figure generation was performed within the R environment (R Core Team, 2017). Change in SLA and SD across the two growing seasons was calculated at the accession level as percentage change using adjusted means. SLA increased in all but two accessions across the two years, thus percentage change in SLA was calculated as: $(2017_{SLA}\text{-}2016_{SLA}) / 2017_{SLA} * 100$. SD decreased in all accessions across the two years, thus percentage

change in SD was calculated as: (2016_{SD}-2017_{SD}) / 2016_{SD} * 100. Tests for associations between all pairwise trait interactions were performed using adjusted means from all models and the Pearson's product moment correlation coefficient. Pairwise interactions between specific leaf-level gas exchange traits were further investigated by fitting second-order polynomial equations between traits. Except for Manhattan plots, all figures were generated using the R package ggplot2 (Wickham, 2016). Manhattan plots for all genetic mapping visualization were generated using the R package qqman (Turner, 2017).

Acknowledgments

We thank Victoria Scaven, Anna Dmitrieva, Dylan Allen, Aishwarya Kammala, and Eric Peterson for help with high throughput phenotyping data collection. We thank Jose Antonio Cumbra, Lauren Murphy, and Abigail Garcia for assistance with the manual stomatal counting. We thank Charles Pignon for helpful discussions and assistance with data analysis. The information, data, or work presented herein was funded in part by the Advanced Research Projects Agency-Energy (ARPA-E), U.S. Department of Energy, under Award Number DE-DE-AR0000661. The views and opinions of the authors expressed herein do not necessarily state or reflect those of the United States Government or any agency thereof.

Figure Legends

Figure 1. Demonstration of stomatal counting algorithm. (a) Reflective intensity layer of an optical topometry (OT) measurement of the abaxial epidermis of a sorghum leaf section. (b) OT measurement overlaid with automatic detection of stomata (red). Automatically detected stomata in close proximity are highlighted in green. (c) Association between median stomatal density of samples where stomates have been both manually and automatically counted. 4-6 fields of view were used to calculate the median values for each genotype by manual and automatic methods. A linear model regressing automatic counts on manual counts is fitted (red) and the standard error of the model is shown (gray). The associated *p-value* significance threshold and r^2 value of the model are inset.

763 Figure 2. Histograms of variation in adjusted means of (a) Stomatal density (SD), (b) specific leaf
764 area (SLA), (c) plant height (g_s), (d) above-ground biomass (A_N), (e) net photosynthesis (A_N), (f)
765 stomatal conductance (g_s). (g) intrinsic water use efficiency (*iWUE*), and (h) ratio of intracellular
766 to atmospheric CO2 concentration (c_i/c_a). The dashed vertical lines denote the population
767 mean.
768
769
770 Figure 3. Correlogram for all measured parameters. Where appropriate, the associated model
771 from which predicted means were extracted is indicated in parenthesis. Traits are arranged
772 according to the angular order of eigenvalues. The color of each individual square describes the
773 Pearson's correlation coefficient (*r*) of each pairwise interaction. Significant correlations are
774 denoted at the level of 0.001 (***), 0.01 (**), and 0.05 (*). Correlations between traits
775 extracted from each individual environment model are listed in Table S2.
776
777 Figure 4. Relationships between gas exchange-related traits. All data are adjusted means. (a)
778 Relationship between stomatal conductance (g_s) and net photosynthesis (A_n). (b) Relationship
779 between An and intrinsic water use efficiency (*iWUE*). (c) Relationship between g_s and *iWUE*.
780 For each relationship, a second-order polynomial model regressing y on x is fitted (blue) and the
781 associated standard error of the model is highlighted (gray). The associated *p-value* significance
782 threshold and r^2 values for each model are inset.
783
784 Figure 5. Bar plot of heritabilities of stomatal density (SD), specific leaf area (SLA), stomatal
785 conductance (g_s), net photosynthesis (A_N), the ratio of intracellular to extracellular CO2 (c_i/c_a),
786 and intrinsic water use efficiency (*iWUE*). Models combining individual and joint yearly data
787 were used to estimate heritability for SD and SLA. Gas exchange traits were only measured in
788 2017.
789
790 Figure 6. Manhattan plots for stomatal density (SD) in 2016 for: (a) GWAS; (b) TWAS in growing
791 point (GP) tissue; (c) TWAS in the third leaf (3L); (d) Fisher's combined test results in GP tissue;

(e) Fisher's combined test in 3L tissue; and (f) a five-way Venn diagram highlighting where genes within the top sets of all mapping approaches for SD-2016 are consistently identified. Blue lines indicates the threshold for the genes with the top 1% of -$\log_{10}$ (*p-values*). Genes with known or putative roles in stomatal development are highlighted in green. Table S8 for gene lists related to each test, tissue, year and trait.

Figure 7. (a) Barplot of the number of unique genes identified with higher confidence as potentially underlying variation on a trait-by-trait basis for net photosynthesis (A_N), stomatal conductance (g_s), the ratio of intracellular to extracellular CO2 (c_i/c_a), and intrinsic water use efficiency (*iWUE*), stomatal density (SD), and specific leaf area (SLA). Higher confidence genes were defined as those identified from multiple tests representing independent evidence from either: TWAS only, but in both tissues (blue fill); Fisher's combined test and/or TWAS in both tissues (green fill); or GWAS plus TWAS or Fisher's combined test in one tissue (yellow fill). (b) Barplot of the number of unique genes consistently identified in multiple independent tests across different traits or growing seasons. For reference, the total number of unique genes identified by a parallel trait by trait approach (394, see panel a) is presented in the first bar. See Table S8 for gene lists related to each test, tissue, year and trait.

Supplemental Figure Legends

Supplemental figure 1. Map showing the point of origin of all accessions employed in this study. Accessions are colored according to race. The size of the points indicates the number of accessions from common origins. The inset biplot shows the genetic structure of all accessions according to principle component analyses.

Supplemental figure 2. Combined line and bar plots of key climate parameters during the growing season of (a) 2016 and (b) 2017. Each plot describes the daily precipitation (blue bars) and maximum daily temperature (red line) from the last week of May until the last week of September. For each year, the total precipitation and average maximum temperature are provided.

Supplemental figure 3. Overview of the custom stomata counting software method. (a) Raw image of sorghum leaf surface with a stoma circled. (b) Enlargement of a disc containing a stoma. A FFT process extracted image features at a series of 25 radii, only three of which are indicated with magenta circles. PCA decomposition of the FFT phase and amplitude values extracted from expert-labeled stomata discs were used to train 9 different machine learning algorithms, each of which produced a pixel value representing probability of belonging to a stoma. (c) Example of a stoma probability map from one of the machine learning methods. A fusion process combined the 9 probability maps and optimized filter parameters to produce a binary classifier that assigned each pixel to a stoma or not-stoma class. (d) A final binary stomata map from which counts were obtained.

Supplemental figure 4. Manhattan plot demonstrating results of GWAS, TWAS, and fisher combined GWAS and TWAS of stomatal density (SD; 2017 model)

Supplemental figure 5. Manhattan plot demonstrating results of GWAS, TWAS, and fisher combined GWAS and TWAS of stomatal (SD; Joint model)

Supplemental figure 6. Manhattan plot demonstrating results of GWAS, TWAS, and fisher combined GWAS and TWAS of specific leaf area (SLA; 2016 model)

Supplemental figure 7. Manhattan plot demonstrating results of GWAS, TWAS, and fisher combined GWAS and TWAS of specific leaf area (SLA; 2017 model)

Supplemental figure 8. Manhattan plot demonstrating results of GWAS, TWAS, and fisher combined GWAS and TWAS of specific leaf area (SLA; joint model)

Supplemental figure 9. Manhattan plot demonstrating results of GWAS, TWAS, and fisher combined GWAS and TWAS of stomatal conductance (g_s)

Supplemental figure 10. Manhattan plot demonstrating results of GWAS, TWAS, and fisher combined GWAS and TWAS of net photosynthesis (A_N)

Supplemental figure 11. Manhattan plot demonstrating results of GWAS, TWAS, and fisher combined GWAS and TWAS of intrinsic water use efficiency (*iWUE*)

Supplemental figure 12. Manhattan plot demonstrating results of GWAS, TWAS, and fisher combined GWAS and TWAS of the ratio of intracellular to atmospheric CO2 concentrations (c_i/c_a)

Supplemental figure 13. Flow chart demonstrating the phenotyping pipeline employed in this study during the 2017 field season. In 2016, leaf-level gas exchange data were not collected.

Supplemental figure 14. Scatter plots of representative examples of leaf-level gas exchange logged during the phenotyping pipeline. Data points for gas exchange were logged every four seconds for four minutes. The mean for the final 15 data points (highlighted in red) was calculated to achieve sample values for (a) net photosynthesis (A_N), (b) stomatal conductance (g_s), (c) ratio of intracellular to atmospheric concentrations of CO2 (c_i/c_a), and (d) intrinsic water use efficiency (*iWUE*).

Supplemental figure 15. Comparison of plant height at 120 days after planting in 2016 and 2017 (Data from: (Dos Santos et al., 2020)(a) Histograms showing variation in genotypic means of plant height in 2016 and 2017. (b) Correlation between genotypic means for plant height in 2016 and 2017.

Supplemental Tables

Supplemental table 1. List of accessions comprising this study.

878 Supplemental table 2. Pearson's correlation coefficients and *p-values* for associations between
879 all traits
880 Supplemental table 3. Top 0.1% of SNPs identified through GWAS for each trait
881 Supplemental table 4. Genes with linkage disequilibrium of the top 0.1% SNPs identified
882 through GWAS for each trait
883 Supplemental table 5. Top 1% of genes identified through TWAS for each trait and each tissue
884 type
885 Supplemental table 6. Top 1% of genes identified through Fisher combined GWAS-TWAS for
886 each trait and each tissue type
887 Supplemental table 7. Tall version of genes identified in the top sets of all mapping approaches.
888 The mapping approach and trait for which they were identified is listed.
889 Supplemental table 8. Wide version of genes identified in the top sets of all mapping
890 approaches. The mapping approach and trait for which they were identified is listed.
891 Supplemental Table 9. List of candidate genes with known or putative roles associated to the
892 traits for which they were identified
893 Supplemental table 10. List of models mixed models used in this study to obtain adjusted
894 genotypic means for all traits
895 Supplemental table 11. Adjusted genotypic means for all traits comprising this study

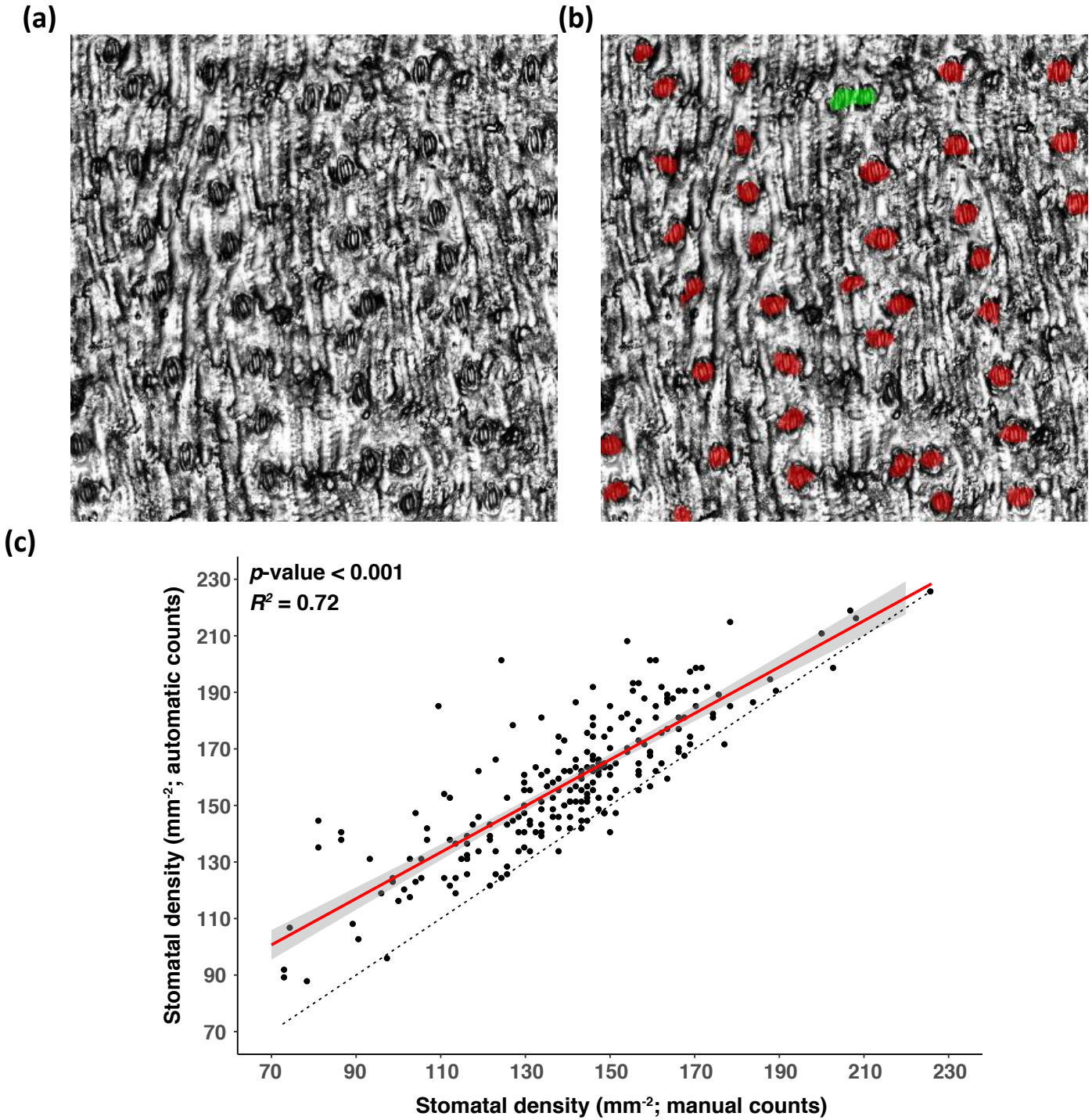
(a)
(b)
(c)
p-value < 0.001
R² = 0.72
Stomatal density (mm⁻²; automatic counts)
Stomatal density (mm⁻²; manual counts)
70
90
110
130
150
170
190
210
230

Figure 1.

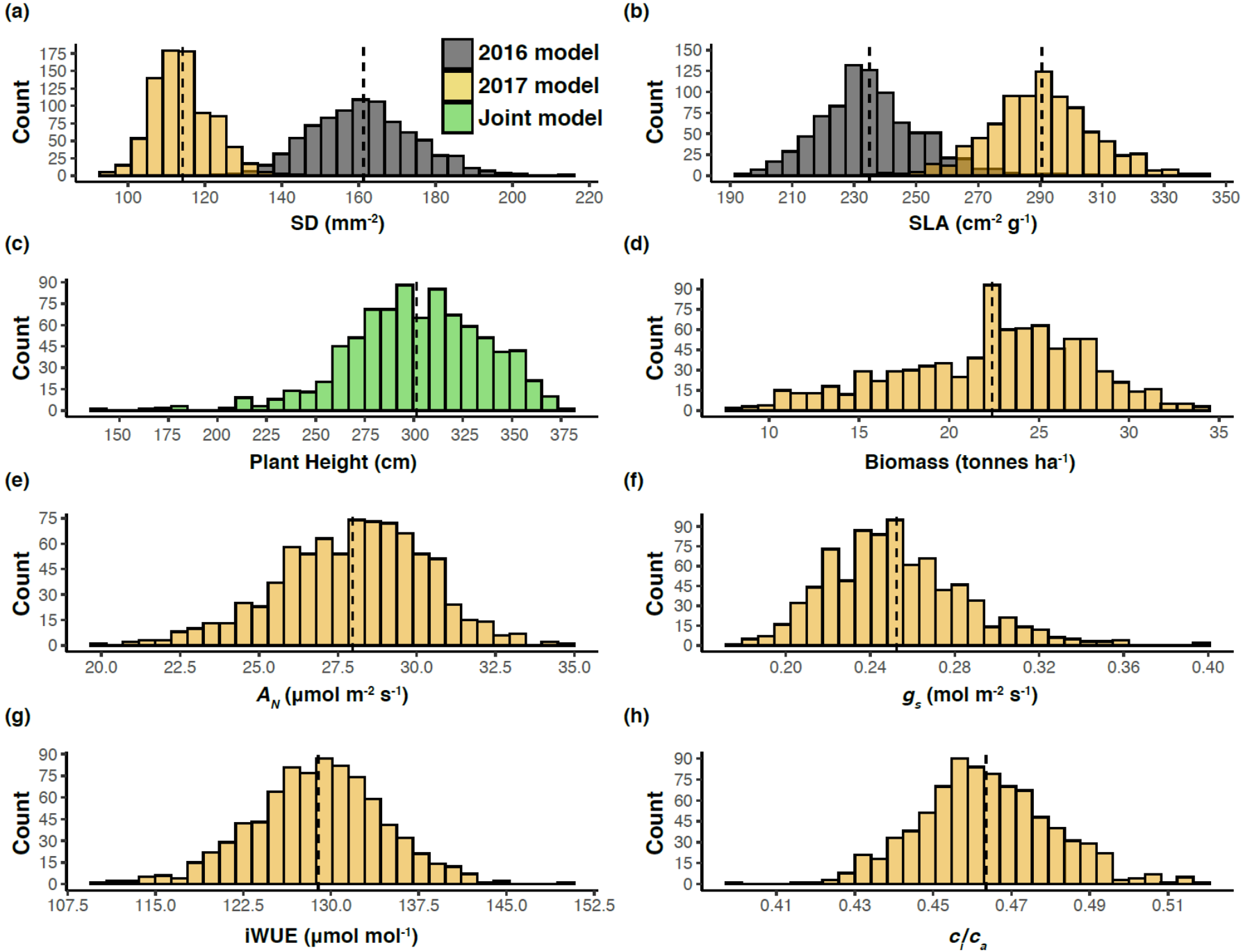
(a)
2016 model
2017 model
Joint model
Count
SD (mm-2)
(b)
SLA (cm-2 g-1)
(c)
Plant Height (cm)
(d)
Biomass (tonnes ha-1)
(e)
AN (µmol m-2 s-1)
(f)
gs (mol m-2 s-1)
(g)
iWUE (µmol mol-1)
(h)
ci/ca

Figure 2.

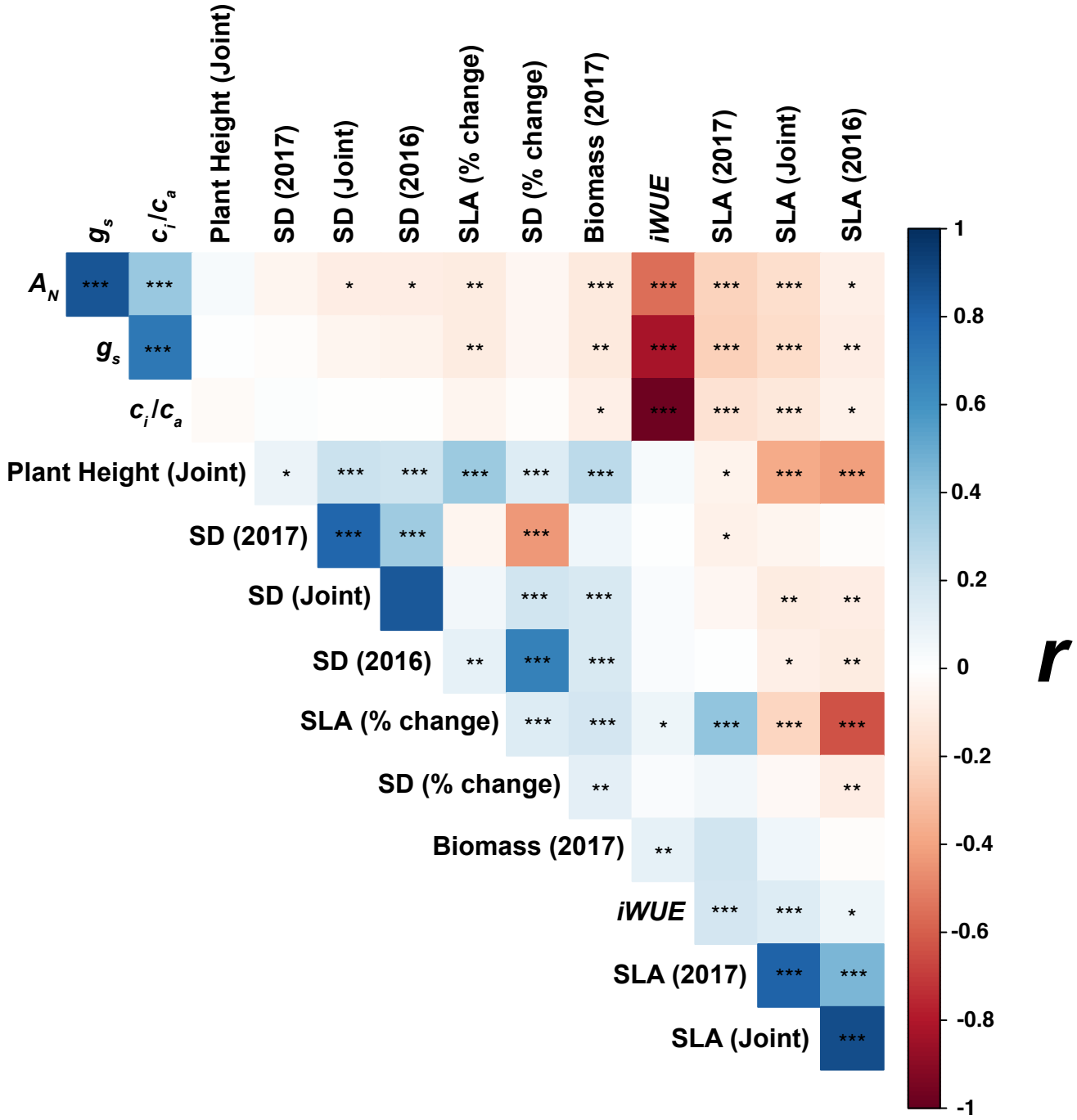
A_N
g_s
c_i/c_a
Plant Height (Joint)
SD (2017)
SD (Joint)
SD (2016)
SLA (% change)
SD (% change)
Biomass (2017)
iWUE
SLA (2017)
SLA (Joint)
SLA (2016)
r
1
0.8
0.6
0.4
0.2
0
-0.2
-0.4
-0.6
-0.8
-1

Figure 3.

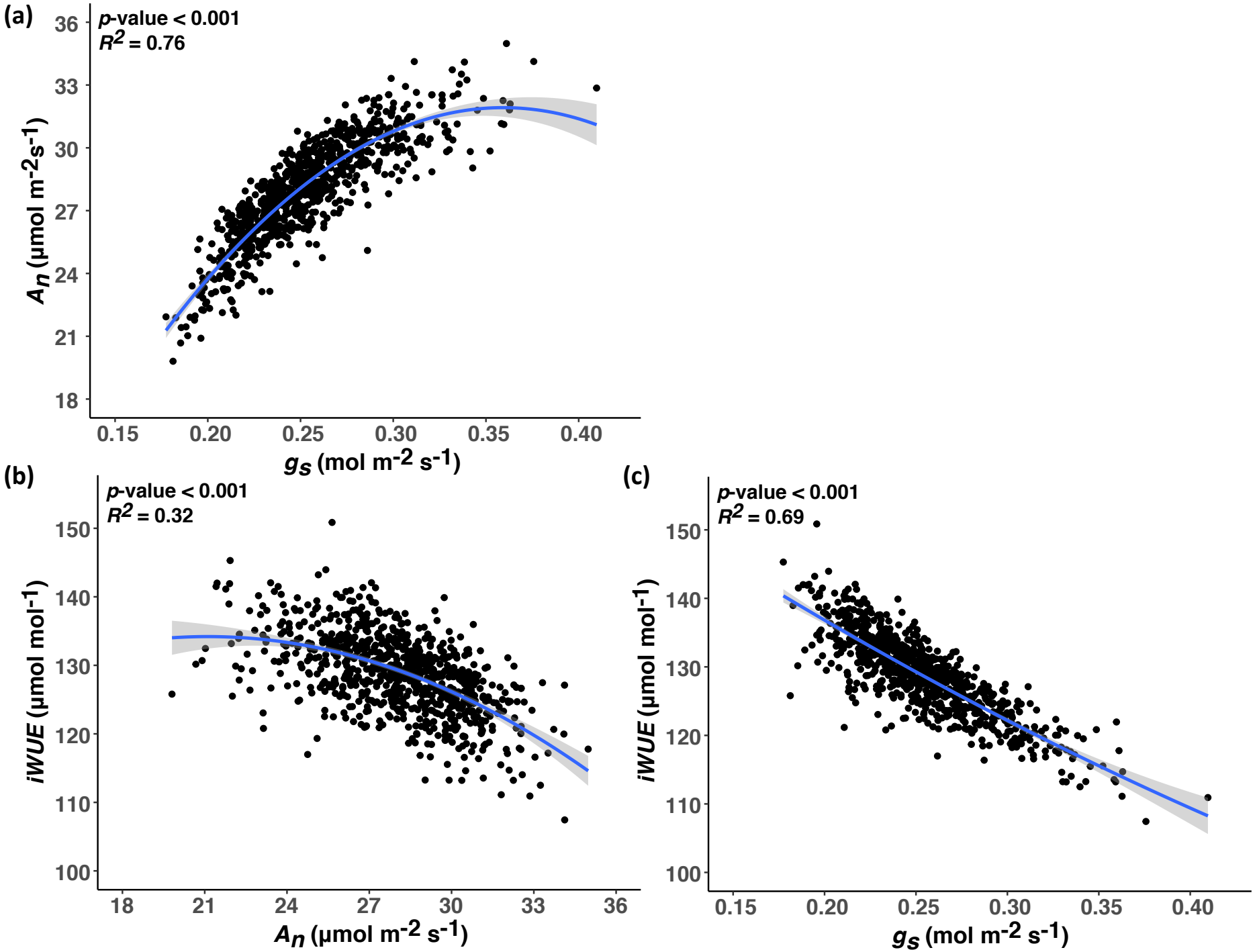
(a)
p-value < 0.001
R2 = 0.76
An (µmol m-2s-1)
gs (mol m-2 s-1)
(b)
p-value < 0.001
R2 = 0.32
iWUE (µmol mol-1)
An (µmol m-2 s-1)
(c)
p-value < 0.001
R2 = 0.69
iWUE (µmol mol-1)
gs (mol m-2 s-1)

Figure 4.

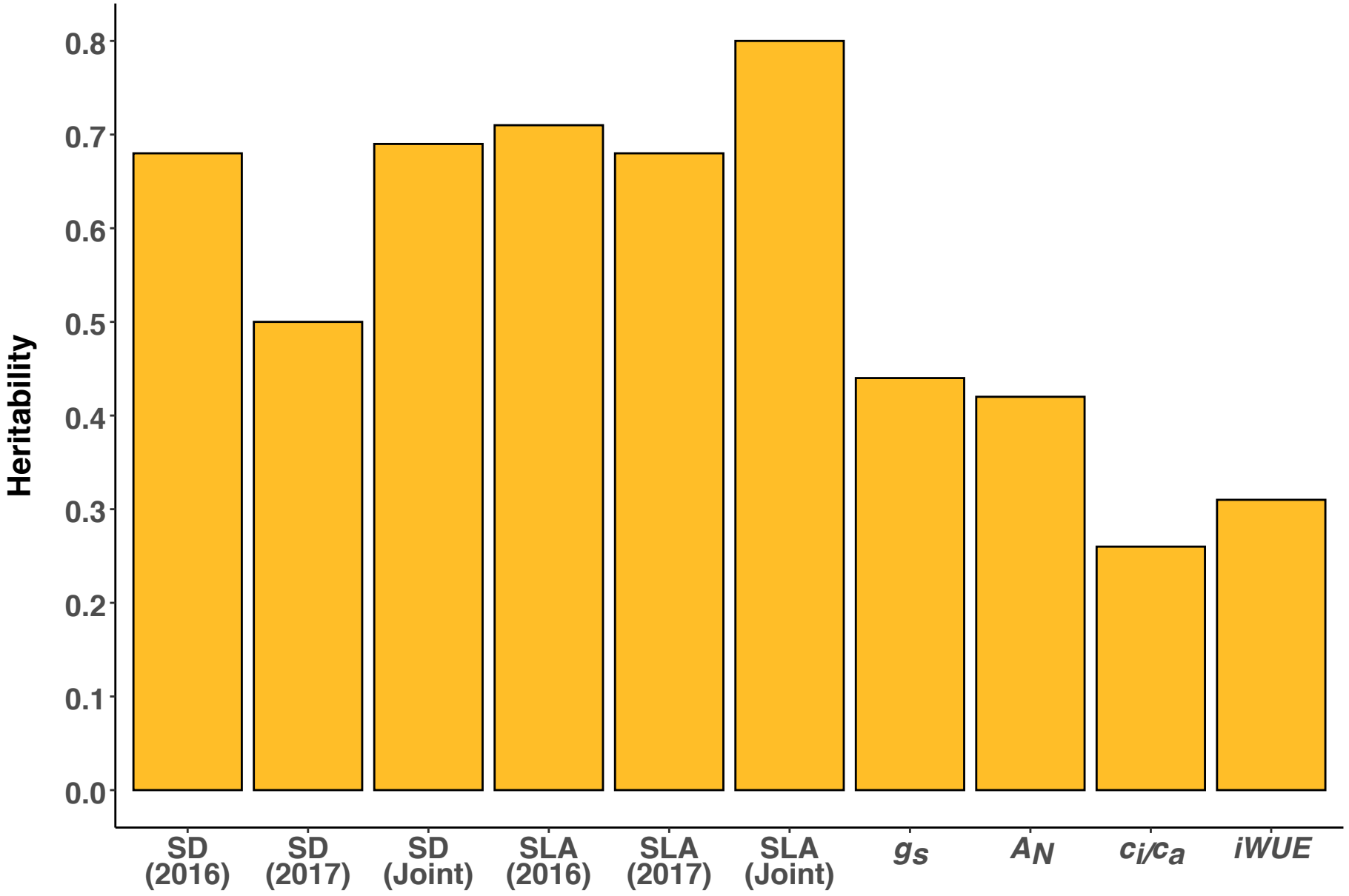
Heritability
0.0
0.1
0.2
0.3
0.4
0.5
0.6
0.7
0.8
SD (2016)
SD (2017)
SD (Joint)
SLA (2016)
SLA (2017)
SLA (Joint)
g_s
A_N
c_i/c_a
iWUE

Figure 5.

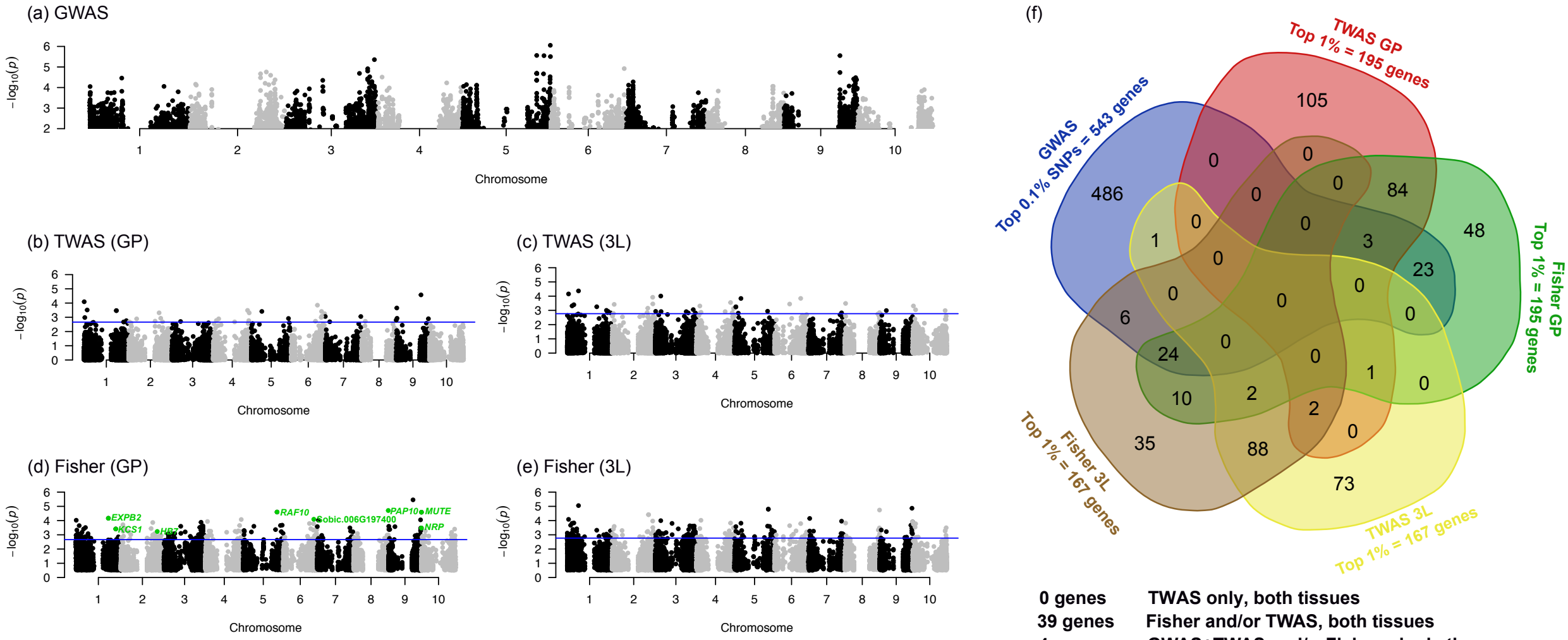
(a) GWAS
(b) TWAS (GP)
(c) TWAS (3L)
(d) Fisher (GP)
(e) Fisher (3L)
(f)
−log10(p)
Chromosome
EXPB2
KCS1
HB7
RAF10
Sobic.006G197400
PAP10
MUTE
NRP
GWAS
Top 0.1% SNPs = 543 genes
TWAS GP
Top 1% = 195 genes
Fisher GP
Top 1% = 195 genes
Fisher 3L
Top 1% = 167 genes
TWAS 3L
Top 1% = 167 genes
486
105
84
48
23
3
1
6
24
10
35
88
73
0 genes TWAS only, both tissues
39 genes Fisher and/or TWAS, both tissues
4 genes GWAS+TWAS and/orFisher, single tissue

Figure 6.

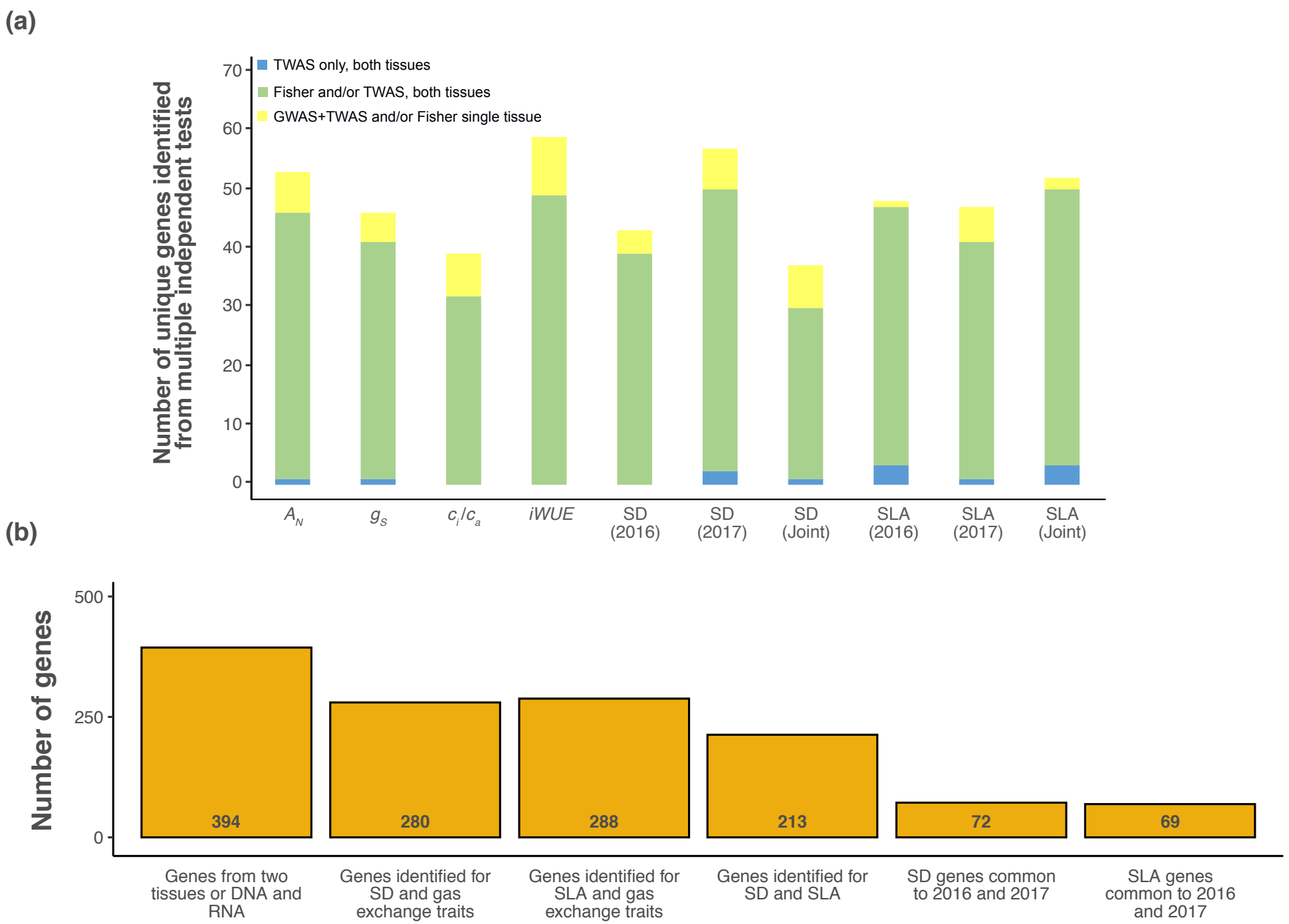
(a)
TWAS only, both tissues
Fisher and/or TWAS, both tissues
GWAS+TWAS and/or Fisher single tissue
Number of unique genes identified from multiple independent tests
70
60
50
40
30
20
10
0
A_N
g_S
c_i/c_a
iWUE
SD (2016)
SD (2017)
SD (Joint)
SLA (2016)
SLA (2017)
SLA (Joint)
(b)
Number of genes
500
250
0
394
280
288
213
72
69
Genes from two tissues or DNA and RNA
Genes identified for SD and gas exchange traits
Genes identified for SLA and gas exchange traits
Genes identified for SD and SLA
SD genes common to 2016 and 2017
SLA genes common to 2016 and 2017

Figure 7.

Parsed Citations

Abrash E, Anleu Gil MX, Matos JL, Bergmann DC (2018) Conservation and divergence of YODA MAPKKK function in regulation of grass epidermal patterning. Development. doi: 10.1242/dev.165860
Google Scholar: Author Only Title Only Author and Title

Ackerly D (2004) Functional Strategies of Chaparral Shrubs in Relation to Seasonal Water Deficit and Disturbance. Ecological Monographs 74: 25–44
Google Scholar: Author Only Title Only Author and Title

Anderson VJ, Briske DD (1990) Stomatal Distribution, Density and Conductance of Three Perennial Grasses Native to the Southern True Prairie of Texas. American Midland Naturalist 123: 152
Google Scholar: Author Only Title Only Author and Title

Atkinson JA, Lobet G, Noll M, Meyer PE, Griffiths M, Wells DM (2017) Combining semi-automated image analysis techniques with machine learning algorithms to accelerate large-scale genetic studies. Gigascience 6: 1–7
Google Scholar: Author Only Title Only Author and Title

Bailey-Serres J, Parker JE, Ainsworth EA, Oldroyd GED, Schroeder JI (2019) Genetic strategies for improving crop yields. Nature 575: 109–118
Google Scholar: Author Only Title Only Author and Title

Berriri S, Garcia AV, Frei dit Frey N, Rozhon W, Pateyron S, Leonhardt N, Montillet J-L, Leung J, Hirt H, Colcombet J (2012) Constitutively active mitogen-activated protein kinase versions reveal functions of Arabidopsis MPK4 in pathogen defense signaling. Plant Cell 24: 4281–4293
Google Scholar: Author Only Title Only Author and Title

Bertolino LT, Caine RS, Gray JE (2019) Impact of Stomatal Density and Morphology on Water-Use Efficiency in a Changing World. Front Plant Sci 10: 225
Google Scholar: Author Only Title Only Author and Title

Caine RS, Yin X, Sloan J, Harrison EL, Mohammed U, Fulton T, Biswal AK, Dionora J, Chater CC, Coe RA, et al (2019) Rice with reduced stomatal density conserves water and has improved drought tolerance under future climate conditions. New Phytol 221: 371–384
Google Scholar: Author Only Title Only Author and Title

Casson SA, Franklin KA, Gray JE, Grierson CS, Whitelam GC, Hetherington AM (2009) phytochrome B and PIF4 regulate stomatal development in response to light quantity. Curr Biol 19: 229–234
Google Scholar: Author Only Title Only Author and Title

Casson SA, Hetherington AM (2010) Environmental regulation of stomatal development. Curr Opin Plant Biol 13: 90–95
Google Scholar: Author Only Title Only Author and Title

Castro FMR, Bruzi AT, Nunes JAR, Parrella RAC, Lombardi GMR, Albuquerque CJB, Lopes M (2015) Agronomic and energetic potential of biomass sorghum genotypes. Am J Plant Sci 6:1862–1873
Google Scholar: Author Only Title Only Author and Title

Chang CC, Chow CC, Tellier LC, Vattikuti S, Purcell SM, Lee JJ (2015) Second-generation PLINK: rising to the challenge of larger and richer datasets. Gigascience 4: 7
Google Scholar: Author Only Title Only Author and Title

Chao Y, Kang J, Zhang T, Yang Q, Gruber MY, Sun Y (2014) Disruption of the homogentisate solanesyltransferase gene results in albino and dwarf phenotypes and root, trichome and stomata defects in Arabidopsis thaliana. PLoS One 9: e94031
Google Scholar: Author Only Title Only Author and Title

Chapin FS (1991) Integrated Responses of Plants to Stress. BioScience 41: 29–36
Google Scholar: Author Only Title Only Author and Title

Chater CCC, Caine RS, Fleming AJ, Gray JE (2017) Origins and Evolution of Stomatal Development. Plant Physiol 174: 624–638
Google Scholar: Author Only Title Only Author and Title

Chelli S, Canullo R, Campetella G, Schmitt AO, Bartha S, Cervellini M, Wellstein C (2016) The response of sub-Mediterranean grasslands to rainfall variation is influenced by early season precipitation. Applied Vegetation Science 19: 611–619
Google Scholar: Author Only Title Only Author and Title

Choquette NE, Ogut F, Wertin TM, Montes CM, Sorgini CA, Morse AM, Brown PJ, Leakey ADB, McIntyre LM, Ainsworth EA (2019) Uncovering hidden genetic variation in photosynthesis of field-grown maize under ozone pollution. Glob Chang Biol 25: 4327–4338
Google Scholar: Author Only Title Only Author and Title

Cornelius C, Leingärtner A, Hoiss B, Krauss J, Steffan-Dewenter I, Menzel A (2013) Phenological response of grassland species to manipulative snowmelt and drought along an altitudinal gradient. J Exp Bot 64: 241–251
Google Scholar: Author Only Title Only Author and Title

Corratgé-Faillie C, Lacombe B (2017) Substrate (un)specificity of Arabidopsis NRT1/PTR FAMILY (NPF) proteins. J Exp Bot 68: 3107–

3113
Google Scholar: Author Only Title Only Author and Title

Cowan IR, Farquhar GD (1977) Stomatal function in relation to leaf metabolism and environment. Symp Soc Exp Biol 31: 471–505
Google Scholar: Author Only Title Only Author and Title

Cullis BR, Smith AB, Coombes NE (2006) On the design of early generation variety trials with correlated data. Journal of Agricultural, Biological, and Environmental Statistics 11: 381–393
Google Scholar: Author Only Title Only Author and Title

DeLucia EH, Chen S, Guan K, Peng B, Li Y, Gomez-Casanovas N, Kantola IB, Bernacchi CJ, Huang Y, Long SP, et al (2019) Are we approaching a water ceiling to maize yields in the United States? Ecosphere. doi: 10.1002/ecs2.2773
Google Scholar: Author Only Title Only Author and Title

Ding S, Zhang B, Qin F (2015) Arabidopsis RZFP34/CHYR1, a Ubiquitin E3 Ligase, Regulates Stomatal Movement and Drought Tolerance via SnRK2.6-Mediated Phosphorylation. Plant Cell 27: 3228–3244
Google Scholar: Author Only Title Only Author and Title

Dittberner H, Korte A, Mettler-Altmann T, Weber APM, Monroe G, de Meaux J (2018) Natural variation in stomata size contributes to the local adaptation of water-use efficiency in Arabidopsis thaliana. Mol Ecol 27: 4052–4065
Google Scholar: Author Only Title Only Author and Title

Dos Santos JPR, Fernandes SB, McCoy S, Lozano R, Brown PJ, Leakey ADB, Buckler ES, Garcia AAF, Gore MA (2020) Novel Bayesian Networks for Genomic Prediction of Developmental Traits in Biomass Sorghum. G3 10: 769–781
Google Scholar: Author Only Title Only Author and Title

Dunn J, Hunt L, Afsharinafar M, Meselmani MA, Mitchell A, Howells R, Wallington E, Fleming AJ, Gray JE (2019) Reduced stomatal density in bread wheat leads to increased water-use efficiency. J Exp Bot 70: 4737–4748
Google Scholar: Author Only Title Only Author and Title

Etherington JR, Pearcy RW, Ehleringer J, Mooney HA, Rundel PW (1990) Plant Physiological Ecology: Field Methods and Instrumentation. The Journal of Ecology 78: 551
Google Scholar: Author Only Title Only Author and Title

Evans JR, Poorter H (2001) Photosynthetic acclimation of plants to growth irradiance: the relative importance of specific leaf area and nitrogen partitioning in maximizing carbon gain. Plant, Cell and Environment 24: 755–767
Google Scholar: Author Only Title Only Author and Title

Feldman MJ, Ellsworth PZ, Fahlgren N, Gehan MA, Cousins AB, Baxter I (2018) Components of Water Use Efficiency Have Unique Genetic Signatures in the Model C Grass. Plant Physiol 178: 699–715
Google Scholar: Author Only Title Only Author and Title

Fernandes SB, Dias KOG, Ferreira DF, Brown PJ (2018) Efficiency of multi-trait, indirect, and trait-assisted genomic selection for improvement of biomass sorghum. Theor Appl Genet 131: 747–755
Google Scholar: Author Only Title Only Author and Title

Foudree A, Aluru M, Rodermel S (2010) PDS activity acts as a rheostat of retrograde signaling during early chloroplast biogenesis. Plant Signal Behav 5: 1629–1632
Google Scholar: Author Only Title Only Author and Title

Franks PJ, Beerling DJ (2009) Maximum leaf conductance driven by CO2 effects on stomatal size and density over geologic time. Proc Natl Acad Sci U S A 106: 10343–10347
Google Scholar: Author Only Title Only Author and Title

Franks PJ, Farquhar GD (2001) The effect of exogenous abscisic acid on stomatal development, stomatal mechanics, and leaf gas exchange in Tradescantia virginiana. Plant Physiol 125: 935–942
Google Scholar: Author Only Title Only Author and Title

Gabriel SB (2002) The Structure of Haplotype Blocks in the Human Genome. Science 296: 2225–2229
Google Scholar: Author Only Title Only Author and Title

Galmés J, Flexas J, Savé R, Medrano H (2007) Water relations and stomatal characteristics of Mediterranean plants with different growth forms and leaf habits: responses to water stress and recovery. Plant and Soil 290: 139–155
Google Scholar: Author Only Title Only Author and Title

Gelaro R, McCarty W, Suárez MJ, Todling R, Molod A, Takacs L, Randles C, Darmenov A, Bosilovich MG, Reichle R, et al (2017) The Modern-Era Retrospective Analysis for Research and Applications, Version 2 (MERRA-2). J Clim 30: 5419–5454
Google Scholar: Author Only Title Only Author and Title

Gonzalez-Paleo L, Ravetta DA (2018) Relationship between photosynthetic rate, water use and leaf structure in desert annual and perennial forbs differing in their growth. Photosynthetica 56: 1177–1187
Google Scholar: Author Only Title Only Author and Title

Gotoh E, Suetsugu N, Higa T, Matsushita T, Tsukaya H, Wada M (2018) Palisade cell shape affects the light-induced chloroplast

movements and leaf photosynthesis. Sci Rep 8: 1472
Google Scholar: Author Only Title Only Author and Title

Gray JE, Holroyd GH, van der Lee FM, Bahrami AR, Sijmons PC, Woodward FI, Schuch W, Hetherington AM (2000) The HIC signalling pathway links CO2 perception to stomatal development. Nature 408: 713–716
Google Scholar: Author Only Title Only Author and Title

Guo F-Q, Young J, Crawford NM (2003) The nitrate transporter AtNRT1.1 (CHL1) functions in stomatal opening and contributes to drought susceptibility in Arabidopsis. Plant Cell 15: 107–117
Google Scholar: Author Only Title Only Author and Title

Hamanishi ET, Thomas BR, Campbell MM (2012) Drought induces alterations in the stomatal development program in Populus. J Exp Bot 63: 4959–4971
Google Scholar: Author Only Title Only Author and Title

Han Y, Gao S, Muegge K, Zhang W, Zhou B (2015) Advanced Applications of RNA Sequencing and Challenges. Bioinform Biol Insights 9: 29–46
Google Scholar: Author Only Title Only Author and Title

Hatfield JL, Dold C (2019) Water-Use Efficiency: Advances and Challenges in a Changing Climate. Frontiers in Plant Science. doi: 10.3389/fpls.2019.00103
Google Scholar: Author Only Title Only Author and Title

Haus MJ, Kelsch RD, Jacobs TW (2015) Application of Optical Topometry to Analysis of the Plant Epidermis. Plant Physiol 169: 946–959
Google Scholar: Author Only Title Only Author and Title

Hepworth C, Turner C, Landim MG, Cameron D, Gray JE (2016) Balancing Water Uptake and Loss through the Coordinated Regulation of Stomatal and Root Development. PLoS One 11: e0156930
Google Scholar: Author Only Title Only Author and Title

Herritt M, Dhanapal AP, Purcell LC, Fritschi FB (2018) Identification of genomic loci associated with 21chlorophyll fluorescence phenotypes by genome-wide association analysis in soybean. BMC Plant Biol 18: 312
Google Scholar: Author Only Title Only Author and Title

Hetherington AM, Ian Woodward F (2003) The role of stomata in sensing and driving environmental change. Nature 424: 901–908
Google Scholar: Author Only Title Only Author and Title

Huang S, Nelson CJ, Li L, Taylor NL, Ströher E, Peteriet J, Millar AH (2015) INTERMEDIATE CLEAVAGE PEPTIDASE55 Modifies Enzyme Amino Termini and Alters Protein Stability in Arabidopsis Mitochondria. Plant Physiol 168: 415–427
Google Scholar: Author Only Title Only Author and Title

Hughes J, Hepworth C, Dutton C, Dunn JA, Hunt L, Stephens J, Waugh R, Cameron DD, Gray JE (2017) Reducing Stomatal Density in Barley Improves Drought Tolerance without Impacting on Yield. Plant Physiol 174: 776–787
Google Scholar: Author Only Title Only Author and Title

Hulshof CM, Violle C, Spasojevic MJ, McGill B, Damschen E, Harrison S, Enquist BJ (2013) Intra-specific and inter-specific variation in specific leaf area reveal the importance of abiotic and biotic drivers of species diversity across elevation and latitude. Journal of Vegetation Science 24: 921–931
Google Scholar: Author Only Title Only Author and Title

Inman-Bamber NG, Jackson PA, Stokes CJ, Verrall S, Lakshmanan P, Basnayake J (2016) Sugarcane for water-limited environments: Enhanced capability of the APSIM sugarcane model for assessing traits for transpiration efficiency and root water supply. Field Crops Research 196: 112–123
Google Scholar: Author Only Title Only Author and Title

Jossier M, Kroniewicz L, Dalmas F, Le Thiec D, Ephritikhine G, Thomine S, Barbier-Brygoo H, Vavasseur A, Filleur S, Leonhardt N (2010) The Arabidopsis vacuolar anion transporter, AtCLCc, is involved in the regulation of stomatal movements and contributes to salt tolerance. Plant J 64: 563–576
Google Scholar: Author Only Title Only Author and Title

Kang C-Y, Lian H-L, Wang F-F, Huang J-R, Yang H-Q (2009) Cryptochromes, phytochromes, and COP1 regulate light-controlled stomatal development in Arabidopsis. Plant Cell 21: 2624–2641
Google Scholar: Author Only Title Only Author and Title

Kapanigowda MH, Perumal R, Djanaguiraman M, Aiken RM, Tesso T, Prasad PV, Little CR (2013) Genotypic variation in sorghum [Sorghum bicolor (L.) Moench] exotic germplasm collections for drought and disease tolerance. Springerplus 2: 650
Google Scholar: Author Only Title Only Author and Title

Kremling KAG, Diepenbrock CH, Gore MA, Buckler ES, Bandillo NB (2019) Transcriptome-Wide Association Supplements Genome-Wide Association in Zea mays. G3: Genes|Genomes|Genetics 9: 3023–3033
Google Scholar: Author Only Title Only Author and Title

Lake JA, Quick WP, Beerling DJ, Woodward FI (2001) Plant development. Signals from mature to new leaves. Nature 411: 154
Google Scholar: Author Only Title Only Author and Title

Lau OS, Song Z, Zhou Z, Davies KA, Chang J, Yang X, Wang S, Lucyshyn D, Tay IHZ, Wigge PA, et al (2018) Direct Control of SPEECHLESS by PIF4 in the High-Temperature Response of Stomatal Development. Curr Biol 28: 1273–1280.e3
Google Scholar: Author Only Title Only Author and Title

Lawson T, Matthews J (2020) Guard Cell Metabolism and Stomatal Function. Annual Review of Plant Biology 71: 273–302
Google Scholar: Author Only Title Only Author and Title

Leakey ADB, Ferguson JN, Pignon CP, Wu A, Jin Z, Hammer GL, Lobell DB (2019) Water Use Efficiency as a Constraint and Target for Improving the Resilience and Productivity of C and C Crops. Annu Rev Plant Biol 70: 781–808
Google Scholar: Author Only Title Only Author and Title

Lee S-J, Lee MH, Kim J-I, Kim SY (2015) Arabidopsis putative MAP kinase kinase kinases Raf10 and Raf11 are positive regulators of seed dormancy and ABA response. Plant Cell Physiol 56: 84–97
Google Scholar: Author Only Title Only Author and Title

Leff B, Ramankutty N, Foley JA (2004) Geographic distribution of major crops across the world. Global Biogeochemical Cycles. doi: 10.1029/2003gb002108
Google Scholar: Author Only Title Only Author and Title

Li L, Wang H, Gago J, Cui H, Qian Z, Kodama N, Ji H, Tian S, Shen D, Chen Y, et al (2015) Harpin Hpa1 Interacts with Aquaporin PIP1;4 to Promote the Substrate Transport and Photosynthesis in Arabidopsis. Sci Rep 5: 17207
Google Scholar: Author Only Title Only Author and Title

Liu X, Chen C-Y, Wang K-C, Luo M, Tai R, Yuan L, Zhao M, Yang S, Tian G, Cui Y, et al (2013) PHYTOCHROME INTERACTING FACTOR3 associates with the histone deacetylase HDA15 in repression of chlorophyll biosynthesis and photosynthesis in etiolated Arabidopsis seedlings. Plant Cell 25: 1258–1273
Google Scholar: Author Only Title Only Author and Title

Liu Y, Dawson W, Prati D, Haeuser E, Feng Y, van Kleunen M (2016) Does greater specific leaf area plasticity help plants to maintain a high performance when shaded? Ann Bot 118: 1329–1336

López-García CM, Ruíz-Herrera LF, López-Bucio JS, Huerta-Venegas PI, Peña-Uribe CA, de la Cruz HR, López-Bucio J (2020) ALTERED MERISTEM PROGRAM 1 promotes growth and biomass accumulation influencing guard cell aperture and photosynthetic efficiency in Arabidopsis. Protoplasma 257: 573–582
Google Scholar: Author Only Title Only Author and Title

Lowry DB, Lovell JT, Zhang L, Bonnette J, Fay PA, Mitchell RB, Lloyd-Reilley J, Boe AR, Wu Y, Rouquette FM Jr, et al (2019) QTL × environment interactions underlie adaptive divergence in switchgrass across a large latitudinal gradient. Proc Natl Acad Sci U S A 116: 12933–12941
Google Scholar: Author Only Title Only Author and Title

Lü H, Yang Y, Li H, Liu Q, Zhang J, Yin J, Chu S, Zhang X, Yu K, Lv L, et al (2018) Genome-Wide Association Studies of Photosynthetic Traits Related to Phosphorus Efficiency in Soybean. Front Plant Sci 9: 1226
Google Scholar: Author Only Title Only Author and Title

Ma L, Li G (2018) FAR1-RELATED SEQUENCE (FRS) and FRS-RELATED FACTOR (FRF) Family Proteins in Growth and Development. Front Plant Sci 9: 692
Google Scholar: Author Only Title Only Author and Title

Marowa P, Ding A, Kong Y (2016) Expansins: roles in plant growth and potential applications in crop improvement. Plant Cell Rep 35: 949–965
Google Scholar: Author Only Title Only Author and Title

Mathur S, Umakanth AV, Tonapi VA, Sharma R, Sharma MK (2017) Sweet sorghum as biofuel feedstock: recent advances and available resources. Biotechnol Biofuels 10: 146
Google Scholar: Author Only Title Only Author and Title

McKown KH, Bergmann DC (2020) Stomatal development in the grasses: lessons from models and crops (and crop models). New Phytol. doi: 10.1111/nph.16450
Google Scholar: Author Only Title Only Author and Title

Meki MN, Ogoshi RM, Kiniry JR, Crow SE, Youkhana AH, Nakahata MH, Littlejohn K (2017) Performance evaluation of biomass sorghum in Hawaii and Texas. Industrial Crops and Products 103: 257–266
Google Scholar: Author Only Title Only Author and Title

Migdal I, Skibior-Blaszczyk R, Heidorn-Czarna M, Kolodziejczak M, Garbiec A, Janska H (2017) AtOMA1 Affects the OXPHOS System and Plant Growth in Contrast to Other Newly Identified ATP-Independent Proteases in Arabidopsis Mitochondria. Front Plant Sci 8: 1543
Google Scholar: Author Only Title Only Author and Title

Mohammed U, Caine RS, Atkinson JA, Harrison EL, Wells D, Chater CC, Gray JE, Swarup R, Murchie EH (2019) Rice plants overexpressing OsEPF1 show reduced stomatal density and increased root cortical aerenchyma formation. Sci Rep 9: 5584

Google Scholar: Author Only Title Only Author and Title

Morison JIL, Baker NR, Mullineaux PM, Davies WJ (2008) Improving water use in crop production. Philos Trans R Soc Lond B Biol Sci 363: 639–658
Google Scholar: Author Only Title Only Author and Title

Movahedi M (2013) Identifying stomatal signalling genes to improve plant water use efficiency. Doctor of Philosophy. The University fo Sheffield
Google Scholar: Author Only Title Only Author and Title

Ohsumi A, Kanemura T, Homma K, Horie T, Shiraiwa T (2007) Genotypic Variation of Stomatal Conductance in Relation to Stomatal Density and Length in Rice (Oryza sativaL.). Plant Production Science 10: 322–328
Google Scholar: Author Only Title Only Author and Title

Ortiz D, Hu J, Salas Fernandez MG (2017) Genetic architecture of photosynthesis in Sorghum bicolor under non-stress and cold stress conditions. J Exp Bot 68: 4545–4557
Google Scholar: Author Only Title Only Author and Title

Pearce DW, Millard S, Bray DF, Rood SB (2006) Stomatal characteristics of riparian poplar species in a semi-arid environment. Tree Physiol 26: 211–218
Google Scholar: Author Only Title Only Author and Title

Pengelly JJL, Sirault XRR, Tazoe Y, Evans JR, Furbank RT, von Caemmerer S (2010) Growth of the C4 dicot Flaveria bidentis: photosynthetic acclimation to low light through shifts in leaf anatomy and biochemistry. J Exp Bot 61: 4109–4122
Google Scholar: Author Only Title Only Author and Title

Pillitteri LJ, Bogenschutz NL, Torii KU (2008) The bHLH protein, MUTE, controls differentiation of stomata and the hydathode pore in Arabidopsis. Plant Cell Physiol 49: 934–943
Google Scholar: Author Only Title Only Author and Title

Podgórska A, Mazur R, Ostaszewska-Bugajska M, Kryzheuskaya K, Dziewit K, Borysiuk K, Wdowiak A, Burian M, Rasmusson AG, Szal B (2020) Efficient Photosynthetic Functioning of Arabidopsis thaliana Through Electron Dissipation in Chloroplasts and Electron Export to Mitochondria Under Ammonium Nutrition. Frontiers in Plant Science. doi: 10.3389/fpls.2020.00103
Google Scholar: Author Only Title Only Author and Title

Qiao P, Lin M, Vasquez M, Matschi S, Chamness J, Baseggio M, Smith LG, Sabuncu MR, Gore MA, Scanlon MJ (2019) Machine Learning Enables High-Throughput Phenotyping for Analyses of the Genetic Architecture of Bulliform Cell Patterning in Maize. G3 9: 4235–4243
Google Scholar: Author Only Title Only Author and Title

Quarrie SA, Jones HG (1977) Effects of Abscisic Acid and Water Stress on Development and Morphology of Wheat. Journal of Experimental Botany 28: 192–203
Google Scholar: Author Only Title Only Author and Title

Qu M, Zheng G, Hamdani S, Essemine J, Song Q, Wang H, Chu C, Sirault X, Zhu X-G (2017) Leaf Photosynthetic Parameters Related to Biomass Accumulation in a Global Rice Diversity Survey. Plant Physiology 175: 248–258
Google Scholar: Author Only Title Only Author and Title

Raissig MT, Matos JL, Anleu Gil MX, Kornfeld A, Bettadapur A, Abrash E, Allison HR, Badgley G, Vogel JP, Berry JA, et al (2017) Mobile MUTE specifies subsidiary cells to build physiologically improved grass stomata. Science 355: 1215–1218
Google Scholar: Author Only Title Only Author and Title

R Core Team (2017) R: A language and environment for statistical computing. R Foundation for Statistical Computing.
Google Scholar: Author Only Title Only Author and Title

Ré DA, Capella M, Bonaventure G, Chan RL (2014) Arabidopsis AtHB7 and AtHB12 evolved divergently to fine tune processes associated with growth and responses to water stress. BMC Plant Biol 14: 150
Google Scholar: Author Only Title Only Author and Title

Sakurai N, Akiyama A, Kuraishi S (1986) Irreversible Effects of Water Stress on Growth and Stomatal Development in Cotyledons of Etiolated Squash Seedlings. Plant and Cell Physiology. doi: 10.1093/oxfordjournals.pcp.a077202
Google Scholar: Author Only Title Only Author and Title

Sara H-C, René G-H, Rosa U-C, Angela K-G, Clelia D-P (2020) Agave angustifolia albino plantlets lose stomatal physiology function by changing the development of the stomatal complex due to a molecular disruption. Mol Genet Genomics 295: 787–805
Google Scholar: Author Only Title Only Author and Title

Scartazza A, Di Baccio D, Bertolotto P, Gavrichkova O, Matteucci G (2016) Investigating the European beech (Fagus sylvatica L.) leaf characteristics along the vertical canopy profile: leaf structure, photosynthetic capacity, light energy dissipation and photoprotection mechanisms. Tree Physiol 36: 1060–1076
Google Scholar: Author Only Title Only Author and Title

Seo DH, Ryu MY, Jammes F, Hwang JH, Turek M, Kang BG, Kwak JM, Kim WT (2012) Roles of four Arabidopsis U-box E3 ubiquitin ligases in negative regulation of abscisic acid-mediated drought stress responses. Plant Physiol 160: 556–568

Google Scholar: Author Only Title Only Author and Title

Shameer S, George Ratcliffe R, Sweetlove LJ (2019) Leaf Energy Balance Requires Mitochondrial Respiration and Export of Chloroplast NADPH in the Light. Plant Physiology 180: 1947–1961
Google Scholar: Author Only Title Only Author and Title

Sheffield J, Wood EF (2008) Projected changes in drought occurrence under future global warming from multi-model, multi-scenario, IPCC AR4 simulations. Climate Dynamics 31: 79–105
Google Scholar: Author Only Title Only Author and Title

Shimizu H, Peng L, Myouga F, Motohashi R, Shinozaki K, Shikanai T (2008) CRR23/NdhL is a subunit of the chloroplast NAD(P)H dehydrogenase complex in Arabidopsis. Plant Cell Physiol 49: 835–842
Google Scholar: Author Only Title Only Author and Title

Shi Y, Wang Z, Meng P, Tian S, Zhang X, Yang S (2013) The glutamate carboxypeptidase AMP1 mediates abscisic acid and abiotic stress responses in Arabidopsis. New Phytol 199: 135–150
Google Scholar: Author Only Title Only Author and Title

Short E, Leighton M, Imriz G, Liu D, Cope-Selby N, Hetherington F, Smertenko A, Hussey PJ, Topping JF, Lindsey K (2018) Epidermal expression of a sterol biosynthesis gene regulates root growth by a non-cell-autonomous mechanism in. Development. doi: 10.1242/dev.160572
Google Scholar: Author Only Title Only Author and Title

Silva EC, Rejane J M, Vale FHA, de Araújo FP, Pimenta MA (2009) Stomatal changes induced by intermittent drought in four umbu tree genotypes. Brazilian Journal of Plant Physiology 21: 33–42
Google Scholar: Author Only Title Only Author and Title

Sinclair TR, Hammer GL, van Oosterom EJ (2005) Potential yield and water-use efficiency benefits in sorghum from limited maximum transpiration rate. Functional Plant Biology 32: 945
Google Scholar: Author Only Title Only Author and Title

Sonawane PD, Pollier J, Panda S, Szymanski J, Massalha H, Yona M, Unger T, Malitsky S, Arendt P, Pauwels L, et al (2017) Corrigendum: Plant cholesterol biosynthetic pathway overlaps with phytosterol metabolism. Nat Plants 3: 17101
Google Scholar: Author Only Title Only Author and Title

Song J, Sun S, Ren H, Grison M, Boutté Y, Bai W, Men S (2019) The SMO1 Family of Sterol 4α-Methyl Oxidases Is Essential for Auxin- and Cytokinin-Regulated Embryogenesis. Plant Physiol 181: 578–594
Google Scholar: Author Only Title Only Author and Title

Tardieu F, Draye X, Javaux M (2017) Root Water Uptake and Ideotypes of the Root System: Whole-Plant Controls Matter. Vadose Zone Journal 16: vzj2017.05.0107
Google Scholar: Author Only Title Only Author and Title

Taylor SH, Lowry DB, Aspinwall MJ, Bonnette JE, Fay PA, Juenger TE (2016) QTL and Drought Effects on Leaf Physiology in Lowland Panicum virgatum. BioEnergy Research 9: 1241–1259
Google Scholar: Author Only Title Only Author and Title

Tian T, Liu Y, Yan H, You Q, Yi X, Du Z, Xu W, Su Z (2017) agriGO v2.0: a GO analysis toolkit for the agricultural community, 2017 update. Nucleic Acids Res 45: W122–W129
Google Scholar: Author Only Title Only Author and Title

Tossi V, Lamattina L, Jenkins GI, Cassia RO (2014) Ultraviolet-B-induced stomatal closure in Arabidopsis is regulated by the UV RESISTANCE LOCUS8 photoreceptor in a nitric oxide-dependent mechanism. Plant Physiol 164: 2220–2230
Google Scholar: Author Only Title Only Author and Title

Truong SK, McCormick RF, Mullet JE (2017) Bioenergy Sorghum Crop Model Predicts VPD-Limited Transpiration Traits Enhance Biomass Yield in Water-Limited Environments. Front Plant Sci 8: 335
Google Scholar: Author Only Title Only Author and Title

Turner SD (2017) qqman: an R package for visualizing GWAS results using Q-Q and manhattan plots. doi: 10.1101/005165
Google Scholar: Author Only Title Only Author and Title

Valluru R, Gazave EE, Fernandes SB, Ferguson JN, Lozano R, Hirannaiah P, Zuo T, Brown PJ, Leakey ADB, Gore MA, et al (2019) Deleterious Mutation Burden and Its Association with Complex Traits in Sorghum (). Genetics 211: 1075–1087
Google Scholar: Author Only Title Only Author and Title

Vicente J, Mendiondo GM, Pauwels J, Pastor V, Izquierdo Y, Naumann C, Movahedi M, Rooney D, Gibbs DJ, Smart K, et al (2019) Distinct branches of the N-end rule pathway modulate the plant immune response. New Phytol 221: 988–1000
Google Scholar: Author Only Title Only Author and Title

Villar R, Marañón T, Quero JL, Panadero P, Arenas F, Lambers H (2005) Variation in relative growth rate of 20 Aegilops species (Poaceae) in the field: The importance of net assimilation rate or specific leaf area depends on the time scale. Plant and Soil 272: 11–27
Google Scholar: Author Only Title Only Author and Title

Vishwakarma A, Bashyam L, Senthilkumaran B, Scheibe R, Padmasree K (2014) Physiological role of AOX1a in photosynthesis and maintenance of cellular redox homeostasis under high light in Arabidopsis thaliana. Plant Physiology and Biochemistry 81: 44–53
Google Scholar: Author Only Title Only Author and Title

Wang C, Liu S, Dong Y, Zhao Y, Geng A, Xia X, Yin W (2016) PdEPF1 regulates water-use efficiency and drought tolerance by modulating stomatal density in poplar. Plant Biotechnol J 14: 849–860
Google Scholar: Author Only Title Only Author and Title

Wang D, LeBauer D, Kling G, Voigt T, Dietze MC (2013) Ecophysiological screening of tree species for biomass production: trade-off between production and water use. Ecosphere 4: art138
Google Scholar: Author Only Title Only Author and Title

Wei H, Luo T, Wu B (2016) Optimal balance of water use efficiency and leaf construction cost with a link to the drought threshold of the desert steppe ecotone in northern China. Ann Bot 118: 541–553
Google Scholar: Author Only Title Only Author and Title

Wellstein C, Poschlod P, Gohlke A, Chelli S, Campetella G, Rosbakh S, Canullo R, Kreyling J, Jentsch A, Beierkuhnlein C (2017) Effects of extreme drought on specific leaf area of grassland species: A meta-analysis of experimental studies in temperate and sub-Mediterranean systems. Glob Chang Biol 23: 2473–2481
Google Scholar: Author Only Title Only Author and Title

Weyers JDB, Travis AJ (1981) Selection and Preparation of Leaf Epidermis for Experiments on Stomatal Physiology. Journal of Experimental Botany 32: 837–850
Google Scholar: Author Only Title Only Author and Title

Wickham H (2016) Programming with ggplot2. Use R! 241–253
Google Scholar: Author Only Title Only Author and Title

Witoń D, Gawroński P, Czarnocka W, Ślesak I, Rusaczonek A, Sujkowska-Rybkowska M, Bernacki MJ, Dąbrowska-Bronk J, Tomsia N, Szechyńska-Hebda M, et al (2016) Mitogen activated protein kinase 4 (MPK4) influences growth in Populus tremula L.×tremuloides. Environmental and Experimental Botany 130: 189–205
Google Scholar: Author Only Title Only Author and Title

Wright IJ, Reich PB, Westoby M (2001) Strategy shifts in leaf physiology, structure and nutrient content between species of high- and low-rainfall and high- and low-nutrient habitats. Functional Ecology 15: 423–434
Google Scholar: Author Only Title Only Author and Title

Xu Z, Zhou G (2008) Responses of leaf stomatal density to water status and its relationship with photosynthesis in a grass. Journal of Experimental Botany 59: 3317–3325
Google Scholar: Author Only Title Only Author and Title

Yates SA, Bruun A, Hodel M, Grieder C, Hund A, Walter A, Studer B (2018) Genetic determination of stomatal patterning in winter wheat (Triticum aestivum L.). bioRxiv. doi: 10.1101/490029
Google Scholar: Author Only Title Only Author and Title

Yuan W, Zheng Y, Piao S, Ciais P, Lombardozzi D, Wang Y, Ryu Y, Chen G, Dong W, Hu Z, et al (2019) Increased atmospheric vapor pressure deficit reduces global vegetation growth. Sci Adv 5: eaax1396
Google Scholar: Author Only Title Only Author and Title

Zhang C, Zhang J, Zhang H, Zhao J, Wu Q, Zhao Z, Cai T (2015) Mechanisms for the relationships between water-use efficiency and carbon isotope composition and specific leaf area of maize (Zea mays L.) under water stress. Plant Growth Regulation 77: 233–243
Google Scholar: Author Only Title Only Author and Title

Zhang C-Z, Zhang J-B, Zhao B-Z, Zhang H, Huang P, Xiao-Peng LI, Qiang-Gen ZHU (2009) Relationships among Water Use Efficiency, Carbon Isotope Discrimination, and Specific Leaf Area in Maize. ACTA AGRONOMICA SINICA 35: 1115–1121
Google Scholar: Author Only Title Only Author and Title

Zhou R, Zhu T, Han L, Liu M, Xu M, Liu Y, Han D, Qiu D, Gong Q, Liu X (2017) The asparagine-rich protein NRP interacts with the Verticillium effector PevD1 and regulates the subcellular localization of cryptochrome 2. J Exp Bot 68: 3427–3440
Google Scholar: Author Only Title Only Author and Title

Zoulias N, Brown J, Rowe J, Casson SA (2020) HY5 is not integral to light mediated stomatal development in Arabidopsis. PLoS One 15: e0222480
Google Scholar: Author Only Title Only Author and Title